norden
Nordic Innovation Centre

February 2011

Soot sensors for efficient combustion and low emissions - SootSensII

- Nanosized soot particles are a serious health hazard in urban air
- Using sensor based thermophoresis and controlled temperature to obtain enhanced deposition of submicron particles

Authors: Anita Lloyd Spetz and Robert Bjorklund

Participants:

Sweden
Linköping University
Prof. Anita Lloyd Spetz

Lund University
Prof. Mehri Sanati

Volvo Technology Corporation/ AB Volvo
Ann Grant

Volvo Car Corporation
Mats Johansson
Advanced engineering Diesel

Mandalon Technologies AB
Per-Erik Fägerman, CEO

SenSiC AB
Lars Hammarlund, CEO

Norway
SINTEF
MSc Andreas Larsson

Finland
Selmic Oy
MSc Jaska Paaso

Romania
”Al. I. Cuza” University of Iasi (UAIC)
Dr Doina Lutic

Title: Soot sensors for efficient combustion and low emissions, SootSensII

Nordic Innovation Centre (NICe) project number: SootSensII 09044

Authors: Anita Lloyd Spetz, Robert Bjorklund and project partners

Institution: Dept. of Physics, Chemistry and Biology, Linköping University

Abstract: Nanosized soot particles are a serious health hazard in urban air. They can penetrate deep into the lungs and their fat solubility makes possible their accumulation in other organs such as the brain. Legislation has therefore continuously reduced allowable emission levels and raised requirements for reporting the status of the exhaust systems including the particulate filter (OBD, on board diagnostics) in diesel powered vehicles.

In this project we developed a sensor based on thermophoresis (patent filed) to enhance soot deposition on the sensor. Thermophoresis is a force acting on particles located in a temperature gradient, such that a sensor held at lower temperatures than the surrounding exhaust gas will obtain enhanced deposition of submicron particles.

Sensors with finger electrodes and a heater for burn off of collected soot were fabricated on one end of alumina substrates (90x5x0.6 mm). A sealed metal tube around the sensor rod (patent filed), which drained heat from the sensor surface allowed a temperature gradient of 30-100°C with respect to the exhaust gas temperature. This sensor layout was further optimized and good results were obtained from several test runs in diesel exhausts. Thermal management has guided the thermos layout. Soot sensors based on a transistor device, employed in the thermos design mounting, were also tested in diesel exhausts. These are especially interesting since soot particles are charged and transistor devices detect charges.

An aerosol based soot generation system was constructed which generated controlled soot atmosphere for testing and calibration of soot sensors in the lab.

Topic / NICe Focus Area: Environmental technology

Key words: Soot, sensor, resistivity measurements, thermophoresis, aerosol technology, diesel exhausts, thermal management, simulation, FET sensors, packaging, sensing layers

ISSN: #	**Language:** English	**Pages: 4**6

Distributed by:
Nordic Innovation Centre
Stensberggata 25
NO-0170 Oslo
Norway

Contact person:
Anita Lloyd Spetz, Prof.
Linköping University
Dept. of Physics, Chemistry and Biology
SE-581 83 Linköping
Sweden
Phone: +47 13 281710
Fax: +47 13137568
E-mail:spetz@ifm.liu.se

Executive summary

Main Objectives:

Nanosized soot particles are a serious health hazard in urban air. Upon inhalation they can penetrate deep into the lungs and their fat solubility makes possible their accumulation in other organs such as the brain. For this reason legislation has continuously reduced the allowable emission levels and raised requirements for reporting the status of the exhaust system (OBD, on board diagnostics) in diesel powered vehicles. To meet the California Air Resources Board proposed legislation for diesel particulate filter, 17.5 mg/mile for light duty vehicles after 2013, will require the development of new sensors for monitoring the exhaust and in particular the status of the particulate filter.

The objective in this project was to further optimize the soot sensor based on thermophoresis, that is a cold sensor surface, for improved sensitivity (patent filed) and to test transistor based sensor structures. The goal was to perform proof of concept of thermophoretic soot sensors in order to get sensor manufacturers to pick up the technology and car manufacturers to implement it. Another goal was to develop an aerosol based soot generation system, by which soot sensors can be tested and calibrated in the laboratory before expensive testing in car and truck engines.

Method / implementation:

Resistivity sensors as well as transistor based sensors were employed to show the potential of thermophoresis to enhance soot deposition on the sensor surface. Thermophoresis is a force acting on particles <100 nm located in a temperature gradient. Since gas molecules coming from the warmer area have a higher velocity than those coming from the cooler, aerosol particles receive a net momentum toward the cooler zone. Thus a sensor surface held at lower temperatures than the surrounding exhaust gas will obtain enhanced deposition of submicron particles and thus achieve higher sensitivities.

Two new batches of sensors with interdigitated finger electrodes (width/gap, 150/100 μm) were fabricated by screen printing PtPdAu conductors on one end of alumina substrates (90x5x0.6 mm). The new designs included improved leads for external connection and an improved heater located under the electrodes for efficient burning off of the collected soot.

Soot particles are known to be charged. Therefore transistor devices are interesting to test as soot sensors. A second batch of transistor devices was processed and subjected to preliminary tests.

A large temperature gradient is required in order for the thermophoresis effect to be efficient. Thermal management of the heat distribution on the sensor surface was used for the design of a “thermos” packaging layout, a sealed metal tube leaving only the finger electrode structure or the transistor protruding into the exhaust gas (patent filed).

A stationary diesel car motor was used to produce exhaust gas. This could be programmed to run in both steady-state and standard driving cycle modes. In both cases soot production was influenced by speed and torque of the engine. Resistance between the fingers or voltage/ current of the transistors and temperature of the sensor and exhaust gas were recorded throughout the measurements.

Aerosol technology was used to produce soot of diesel-like controlled size and concentration in the laboratory. A system for controlled deposition of soot on the sensor surface was constructed. The particle stream had to be quenched in order to generate a controlled size of particles and cooled in order to use the analysis system to quantify and characterize the soot particles. The particle stream was therefore actively heated by a heating gun and the sensor surface was cooled by compressed air. It was also possible to generate soot of only one charge, which should be useful for testing the transistor devices

Concrete results and conclusions:

In this second stage of the project we have processed the second and third batch of soot sensors. The new batches have important improvements, such as functioning conducting leads along the sensor rod, an easy way to implement temperature sensors for precise testing of the technology and an improved heater on the rear side of the alumina rod underneath the finger electrodes/ transistor device for burning off soot. This has been evaluated during three new test runs at VOLVO Technology and VOLVO Cars.

A second batch of transistor devices was processed. However, the change of the layout to circumvent that the soot created a short cut between source and drain did not succeed. Instead a layer of the insulator SU8 was processed and patterned for this purpose. An extra mask was processed at Linköping University.

Cyclic operation with repeated collection (resistance decreases from up to 1 GΩ to <1 MΩ) and burn off steps yielded sensor response curves for different soot concentrations and exhaust gas/sensor temperature combinations. This was perfromed at steady-state conditions for soot concentrations 5-20 mg/m^3 as well as according to the New European and World Harmonized Treansient Driving Cycles required for proof of concept by vehicle manufacturers. The soot sensors were operated in a two temperature cyclic operation mode of detection and soot burn off during the driving cycles. Also, the relationship between the sensor surface temperature and the response time has been shown in order to show the effect of thermophoresis. The transistor devices have been preliminarily tested. Further testing of these interesting devices will be performed in the FunMat Centre, see below.

The aerosol based soot generation system was shown to generate soot particles of similar size as those generated by a diesel engine. It was possible to collect soot in a controlled way on the cold sensor surface. The potential of the system for soot sensor testing and calibration system and the theory of thermophoresis has been carefully described in a recently published article. The SootSensII project was also disseminated in an invited talk

at the International Meeting on Chemical Sensors (IMCS) 2010 in Perth in Australia and in several other conference contributions and journal papers.

Recommendations:

The goal of the SootSens project in the second stage was to realize proof of concept for thermophoresis soot sensor technology and we are very close to this goal. However, we need to quantify the thermophoresis effect a bit further and get a final approval that the sensitivity of the soot sensor is high enough for the requirements of a sensor technology for the OBD application. We hope to reach the goal through one more testing at VOLVO within the FunMat Centre, see below.

When this has been established we are convinced that there is a high possibility that sensor producers will manufacture these soot sensors and car manufacturers will implement the technology in diesel vehicles.

It is important to get the results in the project exposed to the right community and one important conference will be the SAE conference in Detroit, by far the largest technical conference for car industry. The intention is to submit a paper to an SAE conference during 2011. We also have a draft for a (review) paper to Sensors and Actuators B including all most important results from the project. We think the aerosol calibration system, which makes it possible to test and calibrate sensors in the laboratory before expensive tests are run in bench tests on real engines is a strong concept, which should be stressed. It has become important to demonstrate the thermophoretic sensor technology in comparison to our competitors, who have provided VOLVO advanced demonstrators based on both resistivity and charge measuring devices. No-one is, however, (deliberately) using thermophoresis.

Car industry has expressed a special interest in the soot sensor based on transistor devices because these detect the charging from soot particles. The project is also supported by a project at the VINN Excellence Center, FunMat at Linköping University (Lloyd Spetz is deputy director of this center). The transistor devices will be further tested within FunMat, where VOLVO Technology is a partner. Important development of electrical contacts which stands very high temperature and corrosive environment are developed in a project within FunMat. These contacts will in the future be implemented in the soot sensor layout, for finger electrodes and conducting leads.

The coordinator, Lloyd Spetz, started on January 1, 2011 a half time position at Oulu University in Finland as FiDiPro, Finnish Distinguished Professor. The project of this position relates to development of a portable detector in order to detect nanoparticles according to size, shape, concentration and content, since all these parameters have been shown to influence their adverse health effect. The FiDiPro position and its project originates from contacts within the projects SootSens I and II and the achieved results. This will be a much larger project, which will require extensive development of the technology. However, the new project will greatly benefit from the results and methodology built up in the soot sensor project.

Table of contents

Introduction

Health effects of nanoparticles

Nanosized soot particles are a serious health hazard in urban air. Particles, typically of a size less than 10 or 2.5 μm (PM10 and PM2.5) are of growing concern as they contribute to a variety of health and environmental problems [1, 2]. The harmful consequences of soot on human health include respiratory and cardiovascular effects and the particles may be carcinogenic [3, 4]. Upon inhalation they can penetrate deep into the lungs and their fat solubility makes possible their accumulation in other organs such as the brain. Beside these health issues, soot deposition on buildings and vegetation contributes to their long-term degradation. Fine particles also cause reduction in visibility [5, 6], make lakes and streams acidic, deplete the nutrients in soil, and affect the diversity of ecosystems when settling on ground or water. Moreover, particles have both a direct and indirect effect on the earth's climate by either scattering or absorbing solar radiation and by acting as cloud condensation nuclei [7].

For this reason legislation has continuously reduced the allowable emission levels and raised requirements for reporting the status of the exhaust system (OBD, on board diagnostics) in diesel powered vehicles. To meet the California Air Resources Board proposed legislation for diesel particulate filter, 17.5 mg/mile for light duty vehicles after 2013, will require the development of new sensors for monitoring the exhaust.

Soot Sensor Technologies and Patent survey

Soot particle detection and measurement can be achieved by several methods. What has been described in the patent literature is soot collection on filters followed by the subsequent burn off with carbon dioxide measurement [8, 9], optical detection [10, 11] and the measurement of the electrical resistance of a soot layer deposited between two electrical contacts [12, 13]. None of these patents refers to the thermophoresis phenomenon as a basis for the soot deposition between the electrodes. The resistivity technique has been illustrated for both collection and regenerative burn-off for a sensor exposed to an open diesel flame [14]. Collection on the sensor's surface (interdigitated platinum electrodes on an alumina substrate) was done at 350°C, a temperature high enough to avoid water vapor condensation but low enough to prevent significant soot combustion on the platinum electrodes. The authors did not actively create a temperature gradient between the soot in the gas-phase and the sensor surface, nor did they mention the influence of thermophoresis. No information about the soot deposition mechanism was given. Recently Moos and coworkers published a paper where microwave technology is used to determine the soot load in situ of the particulate filter [15].

Soot sensors are developed to control the function and regeneration of the particle filter in diesel engine vehicles in order to for example avoid overheating due to an overload of soot.

Theory of Thermophoresis (ULUND)

Temperature is an important parameter for collection of aerosol particles. Thermophoresis is a force resulting from a temperature gradient being established in the gas phase [16]. Since gas molecules coming from the warmer area have a higher velocity than those coming from the cooler, aerosol particles receive a net momentum toward the cooler zone. A solid surface at lower temperature than the ambient thus can serve as a precipitator for aerosols.

When a given size distribution of generated soot particles passes through the deposition channel, the particles will be subjected to a force gradient towards the cold surface containing the sensor inducing a thermophoretic velocity, U_{th}. This process is independent of particle size while directly proportional to the temperature gradient in the free molecular regime. In the free molecular regime ($d<\lambda$), the thermophoretic velocity can be described by [16]:

$$v_{th} = -0.55 \frac{\mu_g \nabla T}{\rho_g T_p}$$

where ∇T is the temperature gradient in the deposition channel, T_p is the averge temperature of particle assumed to be same as the gas mean temperature, μ_g stands for the gas dynamic viscosity and ρ_g for the gas density.

Particle deposition mechanisms governed by thermophoresis assumes that the measured temperatures are expected to be the same as the gas temperatures at the hot and cold-plate surfaces inside the deposition channel, producing a temperature gradient of $\Delta T = 1.4x10^5$ (ºC/m) across the deposition channel.

Thermophoresis has been used for size independent deposition of Ag particles from polydisperse aerosols [17] and removal of particles from diesel exhaust [18]. Such high collection efficiencies are not necessary for sensor purposes but the temperature gradient must be sufficient to obtain reasonable response times.

The Overall Goal of the SootSensII project

The objective in this project was to implement the idea of thermophoresis, that is a cold sensor surface, as a soot detecting sensor technology with improved sensitivity (patent filed). The goal was to perform proof of concept of thermophoretic soot sensors in order to get sensor manufacturers to pick up the technology and car manufacturers to implement it. Another goal was to develop an aerosol based soot generation system, by which soot sensors can be tested and calibrated in the laboratory before expensive testing in car and truck engines.

VOLVO concluded that priority number one was to position the soot sensor after the particulate filter in order to indicate soot filter failure.

Soot sensor development (LiU, SenSiC, UAIC)

Pre-project initated by VOLVO

The soot sensor development was originally initiated by VOLVO Technology. Linköping University was invited to participate in a PFF (Programmet För Fordonsforskning (Program for Vehicle Research)) #P29148-1 project run by VOLVO and financed by VINNOVA. In this program VOLVO was testing several prototype soot sensors from different manufacturers. LiU was invited to use their sensor competence in order to develop a soot sensor. LiU involved Lund University as a consultant to use their competence in aerosol technology to construct a soot generation system for sensor testing in the laboratory and sensor calibration.

A project meeting at VOLVO created the idea to use thermorphoresis as a sensor technology. In the first approach Peltier elements were tested for cooling of the sensor surface, but this was not viable. Future development of new materials for Peltier elements may however change that.

The resources in the project were then increased by approval of SootSens I and II. A number of new partners and competences in for example packaging, electronics, sensors and processing of sensors were added to the project and this made it possible to implement the thermophoresis technology in sensors possible to test in diesel exhausts.

The PFF project gave resources for VOLVO to test state of the art soot sensors from different manufacturers including the soot sensors from the present project. Soot sensor manufacturers have improved their technologies and new prototypes have appeared. Today prototypes of both resistive type and those that detect charge have been tested in the project run by VOLVO. Our sensor invention still holds as interesting especially the thermophoretic packaging layout employing a transistor based component, since this device also detects charges.

Resistive sensors (LiU)

Sensors based on resistance change of soot collected on interdigitated electrodes have been introduced [14] where sensitivity depends on the known mechanisms of soot deposition (convection, diffusion, impact and thermophoretic effects (the latter mechanism used actively only in the SootSens I & II project)).

In the present project we started by using finger electrode structures patterned on oxidized silicon wafer at LiU. For the sensors used for measurements in diesel exhausts the electrodes were screen printed on alumina substrates at Selmic Oy, see below. The silicon based substrate for the soot detection consisted of a finger electrode structure of Ti and Au sputter deposited on a thermally oxidized Si substrate, Si / SiO_2 (100 nm)/ Ti (5 nm)/ Au (200 nm). The finger electrode structure on the wafer was obtained using lift-off technology. The width of the electrodes was 80 μm and the two gap distances tested were 80 and 300 μm.

The silicon wafer was then cut into small pieces, each containing a single pair of interdigitated electrodes. These were mounted on a substrate positioned in a 16 pin holder where a Pt 100 sensor (Pt resistor with the resistance 100 Ohm at 0°C) allowed temperature measurement, see Fig. 1. The holder was placed in a sealed cell and exposed to soot containing gas flows produced by aerosol technology at ULUND, as described below.

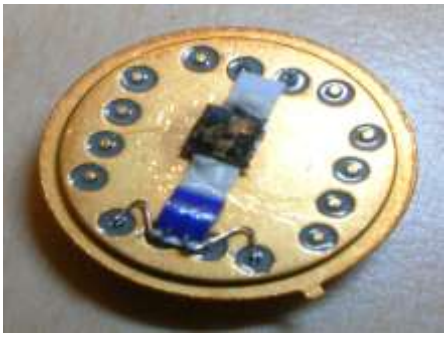

Figure 1. The sensor mounted in a 16 pin header on a substrate (heater) with a Pt 100 temperature sensor (blue)

Sensor Processing by Screenprinting (Selmic Oy)

The sensor will operate in the exhaust pipe of the diesel engine which is an extreme hostile environment. Therefore certain thick film conducting materials were chosen. Expected operating environment was

- Operational: -40 up to +350°
- Storage: -55 ... +125°C
- Harmful substances in the exhaust gas
- Large variation of operating temperature and its cycling nature causes risk of water condensation (since exhausts contains up to 10% water, condensation may occur at temperatures < 100°C)
-

Aluminum oxide substrate and thick film pastes are known to work well in extreme temperatures. Base aluminum oxide (Al_2O_3) substrate is fired over 1300°C and thick film patterns above 850°C. Also a great advantage of these thick films are that the different thick film materials are TCE (Temperature Coefficient of Expansion) matched not only to aluminum oxide substrate but also to each other and that different layers integrates to each other almost seaminglesly which gives great reliability advantage at elevated or lowered temperatures.

The risk of corrosion due to harmful substances in the exhaust gas and risk of electromigration due to condensating water were main drivers when choosing materials

to implement the thick film sensor. Also the selected materials are compliant to ELV – directive [19].

Silver is a commonly used material in thick film applications because of low cost and relatively low electrical resistance. Down side of silver is that it is a very sensitive material in terms of electro migration and emission. Gold is used in applications where high reliability is required. Gold is also not susceptible to ionic migration. A disadvantage of gold is high cost. Copper is also used for thick film conductors but since the copper requires sintering in nitrogen atmosphere it's not compatible with all thick film materials.

The design of prototype sensors at Selmic followed the company specific design rules. Manufacturing was made by using existing equipment and production lines which are also used in volume production. All operations are quality certified according ISO9001-2001 and ISO/TS 16949:2002.

First batch of sensors was made with Au based materials containing also palladium except solid back side metallization on version 2, which was made with silver based conductor. Heater resistors were made in serpentine shape by using special silver containing low ohmic resistor pastes. Everything except the sensitive sensor area was protected with a dense, acid resistant protective overglaze layer.

Three different layout versions were made in the first batch. The main difference between the layouts was the pattern on the backside of the aluminum oxide rod. The first version employed integrated heaters on the backside for the three sensors to be assembled on the top side of the rod. Second version hold solid back side metallization and third version was without any thick film prints on the back side, just pure aluminum oxide.

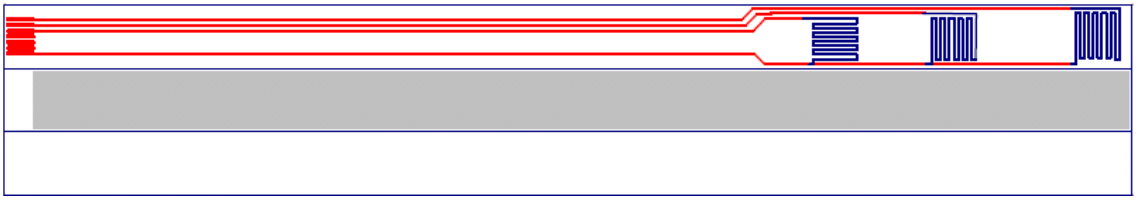

Figure 2. Batch 1, three different rear side sensor layout

1. Rear side with integrated thick film heaters
2. Rear side solid metallization
3. Rear side solid with bare aluminum oxide surface

In the top side design, See Fig. 3, there were spots for bonding three silicon based platinum sensors (red rectangle) and one integrated thick film sensor containing platinum finger electrodes (green rectangle). Also a heater resistor was designed around the top most sensor (yellow rectangle).

Figure 3. Batch 1, top side of the sensor

Figure 4. Batch 1, top side with heater resistor around top most sensor element and spots for three optional silicon substrate sensor elements

Figure 5. Batch 1, thick film sensor element circumvented by heater resistor

Conclusions from batch one was that the thick film sensors detected soot and thus was working but conductor resistance was too high. This was because of too narrow line widths and relatively high sheet resistance of the PtPdAu –paste used.

In batch 2 a new layout was designed based on experiences collected from batch 1. To gain lower conductor resistance from contact pins to sensor element silver based conductors were chosen. All conductor tracks were covered with dense, acid resistant over glaze again. The layout was optimized for only one set up of thick film finger electrodes or optionally silicon based element on top of the rod. This layout gave the possibility to widen conductor lines in order to decrease the conductor resistance. Heaters were removed from the design. The material and layout of the finger electrodes remained unchanged.

Figure 6. Batch 2. Top view of sensor rod with widened conductors

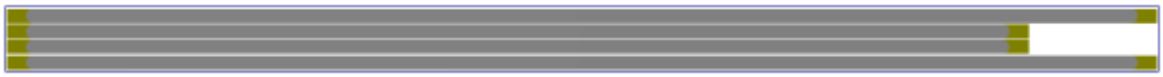

Figure 7. Batch 2. Rear side

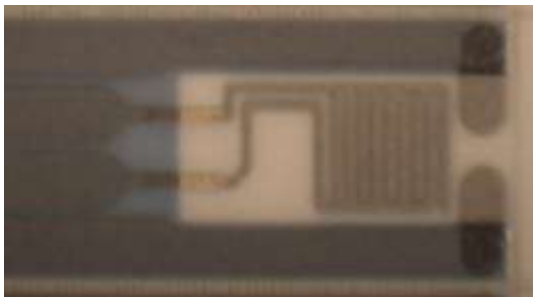

Figure 8. Batch 2. Sensor element terminated with

silver conductors and covered with protective overglaze.

Transistor devices (SenSiC, LiU)

The soot particles are known to be charged, and therefore it is interesting in this project to also investigate the potential of transistor devices as soot sensors. The technology is based on silicon carbide, SiC, transistor devices, since this provides a technology known to be very resistant to high temperature and harsh environment [20]. These devices have been developed for example for combustion control in car exhausts and domestic boilers. The latter technology is now being commercialized by SenSiC AB.

The sensor chips are very small, a 4 inch wafer contains thousands of sensor chips, and therefore the cost is small even though a silicon carbide wafer is quite expensive, see Fig. 9.

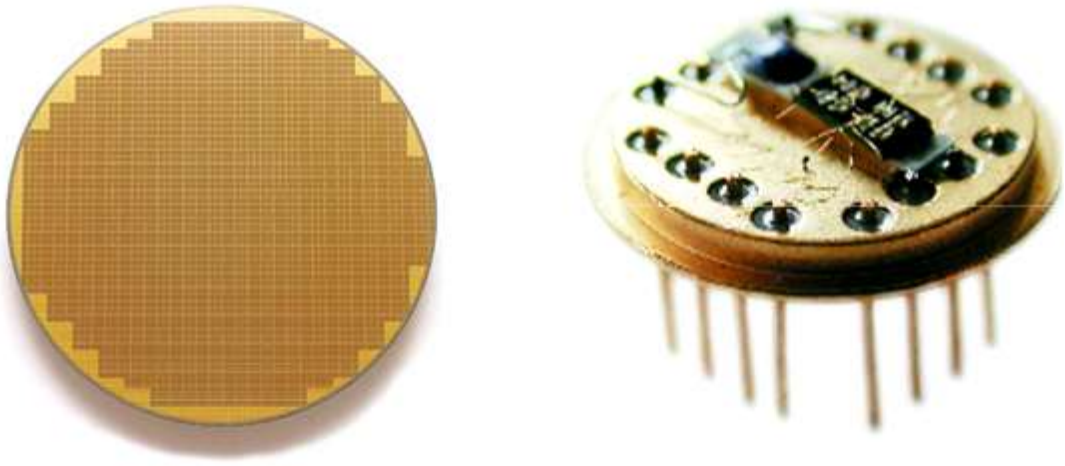

Figure 9. To the left: Silicon carbide wafer, 3 inch in diameter (4 inch available today) , with ~ 1000 sensor chip. To the right: Mounting in a 16 pin holder of one sensor chip and a temperature sensor (blue) on a substrate, which can be heated.

Layout changes will have to be performed of the device design used for gas sensors, otherwise the soot deposition will create a short cut between drain and source. The first batch of transistors, which was processed did not function as soot sensors. Improvement of the design has been performed for the second batch of transistors. Still extra insulation was needed to prevent shortcut between source and drain by deposited soot particles. An extra mask was processed at LiU and SU8 was deposited over the sensor chip and patterned. In this way a suitable opening was created over the transistor gate area by etching SU8.

Sensing layers (UAIC, LiU)

The role of UAIC in the project was to deposit porous layers on the sensitive surface, favoring the soot deposition in the measuring step and its elimination in the regeneration step. The solid materials must have potentially oxidizing activity for the soot (which is a very carbon rich material) and high porosity.

Good candidates for this puspose are small-size semiconductive oxide grains, deposited on mesoporous materials of silica type. SBA-15 silica is a mesoporous material, having a structure made of parallel hollow tubes, packed in a hexagonal arrangement, with thick semi-amorphous pores. The free diameter of the tubes vary from 5 to 20 nm, depending on the surfactant used in the synthesis. The use of P-123, a copolymer of ethylene and propylene oxides, chemical formula $HO(CH_2CH_2O)_{20}(CH_2CH(CH_3)O)_{70}(CH_2CH_2O)_{20}H$ and an average molar mass of 5800, allows obtaining a silica with high surface areas (up to 1200 m^2/g) and thick pore walls, stable under thermal and hydrothermal conditions. Tetraehtyl-orthosilicate was used as the silica precursor. The synthesis consists of the hydrolysis and subsequent condensation of the silica precursor, in aqueous acidic media, by using HCl. The surfactant is trapped inside the structure of the solid and had been removed by slow calcination (1^o/min) for 4 hours, under air, at 550^oC. The porous structure of the solid was confirmed by BET adsorption analysis.

The dopants were deposited by the incipient impregnation technique, using solutions of the precursors as follows:

- indium chloride hydrate, for indium oxide obtaining
- tin (II) chloride hydrate
- hexacloroplatinic acid hydrate

All the solutions of the precursors were prepared by dissolving the salts in ethanol. The impregnation was preformed in three identical steps and the calcination at 400^oC performed after each step allowed the fixation of the oxides and platinum on the walls of the SBA-15 silica. The reason for this repetition was to obtain a fast entrance of the impregnation solutions inside the pores, meaning no solvent remained when the silica dried at 200^oC for 2 hours, minimizing thus the possibility of preferential diffusion and pore narrowing due to the mouth opening (as it happens when big impregnation solution volumes are contacted with the solid). The drying of the silica allowed the adsorption sites to be free and very “greedy” for precursors’ adsorption.
The XRD analysis, see Fig. 10, confirmed that tin oxide and small platinum grains on SBA-15 was obtained and a separate segregate phase of indium oxide. It is worth to note that the mixture of indium and tin precursors led to a phase similar to tin oxide, not indium oxide, although the ratio between In and Sn was 1/1 in the precursors solutions.

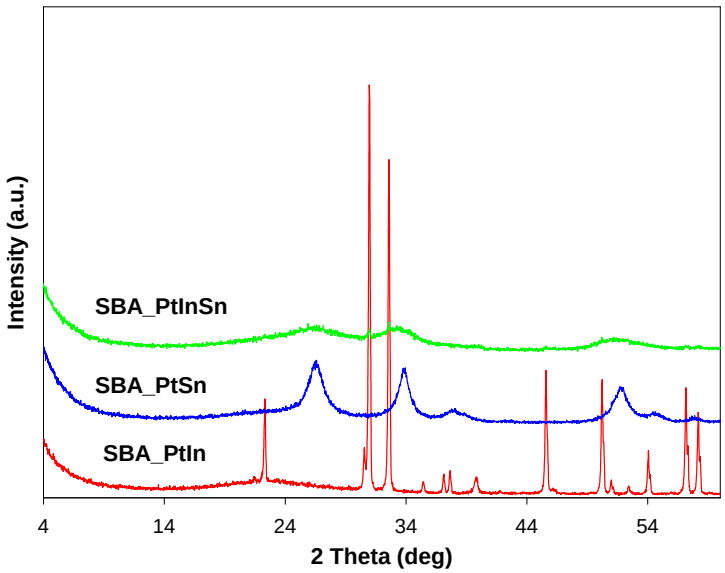

Figure 10. XRD diffraction patterns of SBA-15 based impregnated samples

The BET adsorption analysis, see Fig. 11, performed by pure nitrogen adsorption at 77K showed that the pores shapes and size distribution remained almost unchanged in the case of SBA_PtIn sample, while the SBA_PtSn and SBA_PtInSn samples showed slight pore narrowing, indicating partial entrance of the impregnated oxides inside the SBA-15 pores in the case of the latest two samples. This is proven by the presence of two steps in the desorption branch of the isotherm for the case of SBA_PtSn and SBA_PtInSn samples. The pore size distribution also shows a significant decrease of the maxima position on the curve in connection to the enlargement of the pore size.

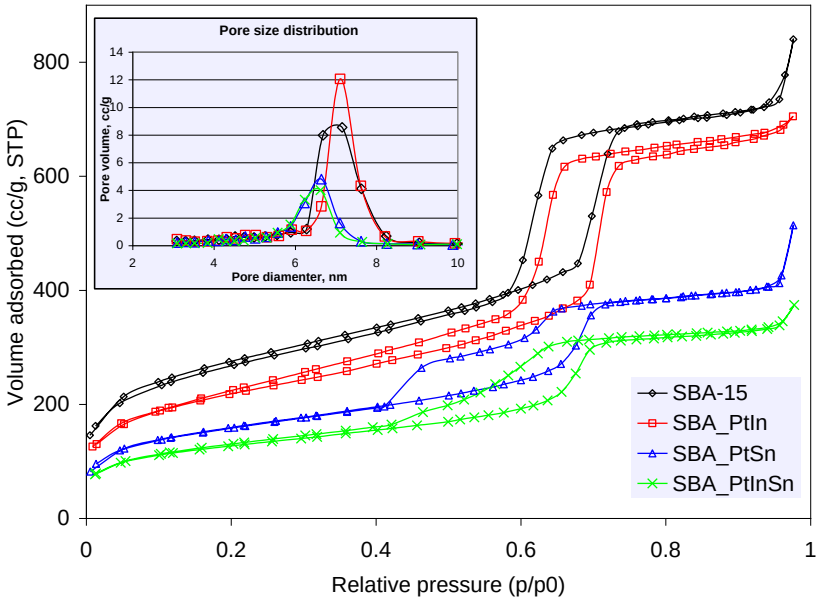

Figure 11. BET adsorption isotherms and pore size distribution for the SBA-15 based impregnated samples

The most difficult problem was to obtain an adherent and stable layer on the sensor exposed to gas flows containing soot. However, neither the casting method (deposition of a drop of suspension of the solid in a solvent) nor including a bonding sticky compound in the slurry (chitosan or carboxymethylcellulose) did not generate satisfactory layers, despite the good structural properties of the solids. Another solution was finally adopted. The sensitive material was deposited directly on the substrate, by imersing the sensing substrate in the precipitation vessel. The method was applied for the precipitation of double-layered structures of anionic clays type (hydrotalcites).

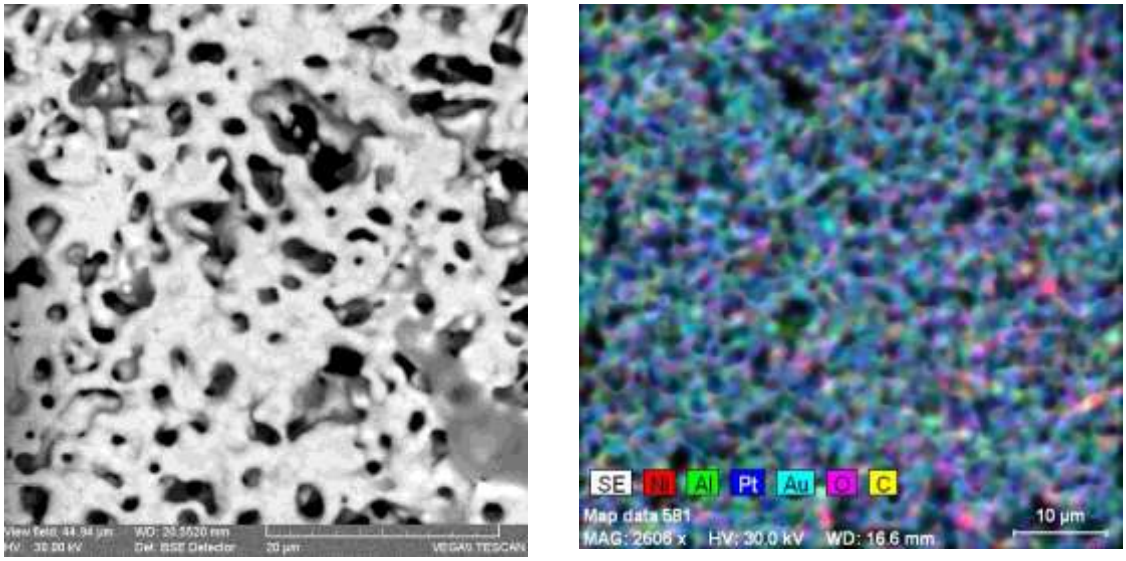

Fig. 12. SEM image of a NiAl hydrotalcite doped with platinum (left). The composition maping for the Ni-Al-Pt-hydrotalcite sample (right).

The synthesis method is not aggressive against the substrate (as for zeolite and mesoporous materials synthesis) and proved to be very effective for thin layer generation. The solid material deposited on the ceramic substrate has a high porosity and uniform distribution of the component elements, as shown in Fig. 12.

Aerosol Technology (ULUND)

Soot generation

Particulate Matter, PM, is a complex mixture of small airborne particles and liquid droplets typically consisting of agglomerates of primary particles (with 20-35 nm diameter) and smaller nucleation mode particles mostly in liquid phase. The primary particles in agglomerates are composed of soot (elemental carbon coated with traces of metallic ash) and onto those agglomerates, the heavier organic compounds and sulphuric acid are condensed. The nucleation mode particles on the other hand are dominated by condensed hydrocarbons and sulfates [21, 22].

The designed combustion soot generator, see Fig. 11, consists of three sections: a diffusion flame, flame quenching and particles mixing. Propane as fuel was fed into the inner of two co-axial stainless steel pipes of 7 and 28 mm i.d., respectively. While particle free dry air (PFA) was introduced through the outer pipe as an oxidant. The stability of the flame, and thus the generated soot, is very sensitive to small variations in the flow pattern. Two mass flow controllers (Bronkhorst High-Tech MFCs) were used to regulate the fuel and coating air flow rates with high precision. Additionally, the coating air stream was stabilized with a ceramic honeycomb monolith acting as a flow laminarizer to further enhance flame stability. By varying the fuel and air flow rates and hence the equivalence ratio, soot particles of different concentrations and size distributions was generated, see Table 1.

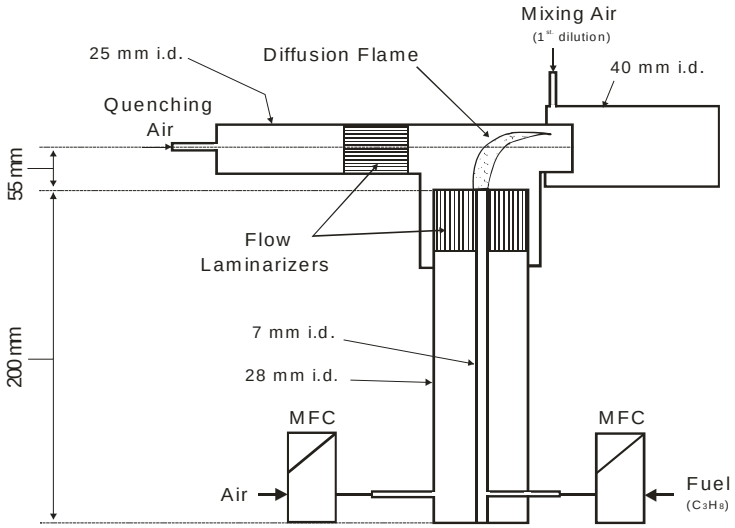

Figure 11**:** Shematic diagram of the experimental set-up

Table 1: Flow rates of fuel and coating air and geometric mean diameter (GMD) of particles produced.

Case	Equivalence ratio ϕ	Fuel / air flow rates (L/min) / (L/min)	Soot particles generated GMD, nm
Equivalence ratio 1	0.632	0.085 / 3.2	55
Equivalence ratio 2	0.653	0.085 / 3.1	85
Equivalence ratio 3	0.675	0.085 / 3.0	110

Thermophoretic soot sampler and deposition on sensor

The next step in this study was to investigate the capability of using thermophoresis as a method to deposit soot particles on the soot sensor and determine the key parameters within deposition and detection steps.

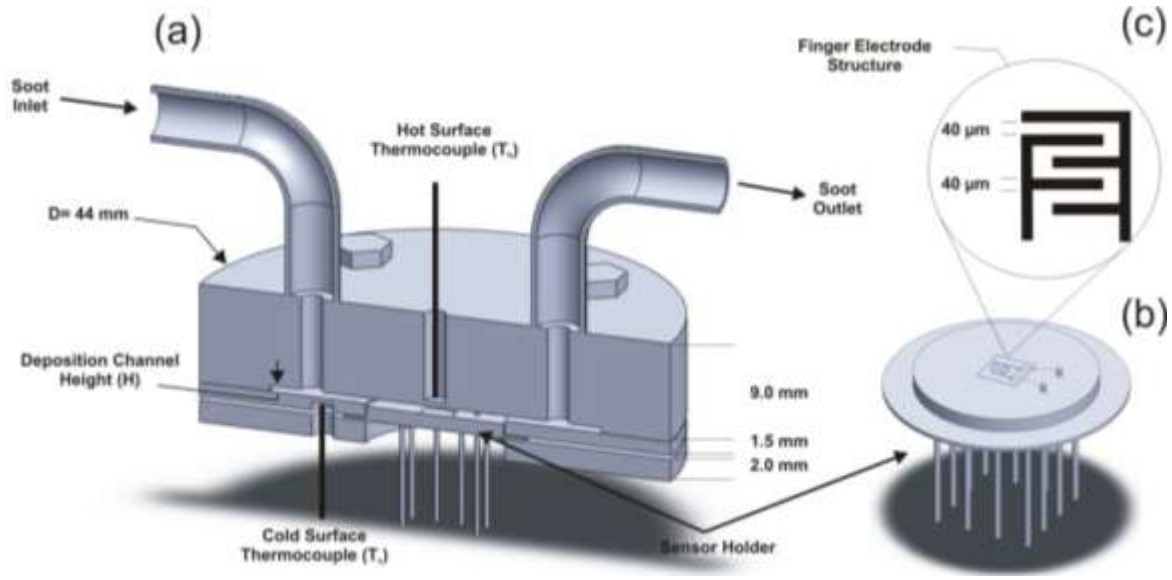

Figure 12: A three-dimensional cross section view of the soot sampler (a) and sensor holder (b) including dimensions of the finger electrode sensor structure (c).

Figure 12 shows the thermophoretic soot sampler that was designed and used for the deposition of generated soot particles on the sensor. The sampler was manufactured based on a plate-to-plate thermal precipitator design [23, 24].

We applied a constant flow rate of 300 ml/min and in all deposition experiments the Reynolds number (Re = 23) indicates a laminar flow. However, as the inlet flow enters the deposition channel perpendicularly, a turbulent flow is expected initially and requires a certain length (hydrodynamic length) to become laminar. The hydrodynamic length can be calculated as

$L_h = 0.04 \cdot Re \cdot D_h$

Where D_h stands for the hydrodynamic diameter of the flow channel calculated as

$D_h = 2W \cdot H/(W+H)$.

Accordingly, $L_h = 0.9$ mm ensures a laminar flow over the sensor. It has been shown in the literature that thermophoretic deposition can be achieved under both laminar and turbulent flow conditions [26]. Moreover, earlier investigation by Tsai and Lu [24] showed that the thermophoretic deposition efficiency is only slightly decreased under turbulent conditions compared to laminar for Re values of 6580 and 1340, respectively.

Messerer et al. [23] showed that the deposition efficiency of agglomerated soot particles in a thermophoretic plate-to-plate deposition cell was within 5%, independent of particle size over the range of 30-300 nm (the size range relevant for this study). We also calculated the thermophoretic velocity and particle collection efficiency using both free molecular regime ($d<\lambda$) and continuum regime formulations (particle size larger than the molecular mean free path; $d>\lambda$). The thermophoretic velocity for $d<\lambda$ was found to be

0.52 cm/s and that for d>λ 0.38 cm/s. The efficiency of particle collection in the deposition cell was found to be 46.4% and 35% for d<λ and d>λ respectively [16].

Soot particle characterization

A scanning mobility particle sizer (SMPS 3934 form TSI Inc., USA) was used to characterize the number size distribution of the generated soot. It consists of a differential mobility analyzer (DMA 3071) and a condensation particle counter (CPC 3010) operating at a sample flow rate of 1.0 l/min and a sheath air flow rate of 6.0 l/min allowing a measurement range of 10-450 nm. Before the generated soot was analyzed with the SMPS system, it was diluted using an ejector diluter with a modified inlet nozzle (DI-1000 Dekati Diluter, Finland) to a ratio of 1:13 in order not to exceed the measurable range for the SMPS. After SMPS verification of a stable size distribution of the generated soot particles, a flow of 300 ml/min was established from the outlet of the burner using a critical orifice at the thermophoretic sampler outlet, see Fig. 13.

Organic and elemental carbon analysis and TEM analysis

The organic and elemental carbon analysis (OC/EC) of the particles was performed by collecting samples on pre-baked quartz fiber filters (Tissue quartz, SKC Inc.) and subsequently analyzed according to the standard thermal method (VDI 2465/2) by a Thermal Carbon Analyzer (Model 2001, Desert Research Instruments Inc.). The set-up for the soot collection involved sampling soot directly from the burner outlet into two parallel lines at the same flow rates. In one line only a quartz filter was used, while in the other line a Teflon filter (Zeflour, SKC Inc.) was followed by another quartz filter. This configuration allows correction for possible gas phase organic vapors absorbed onto the quartz filter.

The morphology of the generated soot particles was investigated by a 60 KeV PHILIPS CM10 Transmission Electron Microscope (TEM) using an electrostatic precipitator (NAS Model 3089, TSI Inc.) whereas the samples were collected on a carbon-coated copper grid of diameter 3 mm.

The Aerosol Particle Mass Analyzer (APM)

The APM coupled in series with a DMA (DMA-APM), was used for online mass determination of mobility classified particles, see Fig. 15. The system can be used for the determination of the particle effective density and mass-mobility relationship. The APM consists of an outer (r_2) and an inner (r_1) cylinder rotating at the same rotational speed ω. The aerosol is introduced in the annual gap between the cylinders and a potential (V_{APM}) applied to the inner cylinder while keeping the outer cylinder grounded. Thus, the force keeping the charged particles in orbit is the electrical force, balanced by the centrifugal force. Since the centrifugal force is mass dependent the particle mass can be determined according to:

$$m = \frac{qE}{r\,\omega^2} = \frac{qV_{APM}}{r^2\omega^2\,\ln(r_2 / r_1)}$$

where r is the average radial distance to the gap between the cylinders from the axis of rotation ($(r_2 - r_1)/2$), q the particle charge and E the electrical field. The APM is described in more detail by McMurry et al. [26].

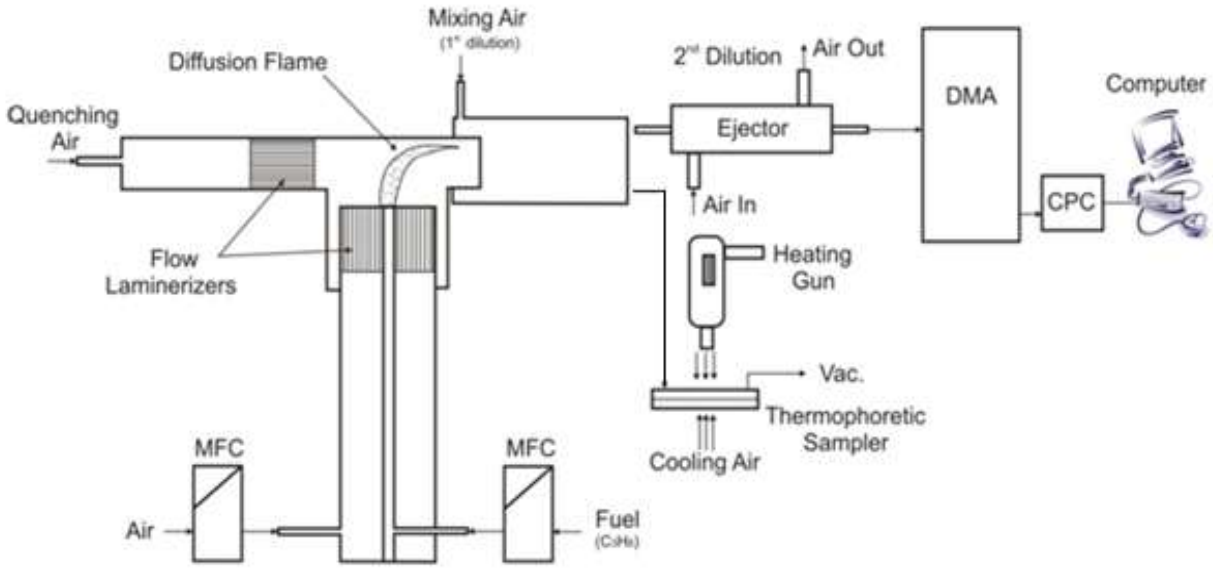

Figure 13. Schematic diagram of the experimental set-up

In the system, a DMA and an APM are coupled in series where the DMA selects particles of one mobility diameter at a time and the mass distribution of the selected particles is determined by stepping the APM voltage. The mobility diameter (d_{me}) and the particle mass are, in the transition regime, related as:

$$m = \underbrace{\frac{\rho}{\chi^3}\cdot\left(\frac{C(d_{me})}{C(d_{ve})}\right)^3}_{\rho_{eff}}\cdot\left(\frac{\pi}{6}\right)\cdot d_{me}^3$$

where ρ_{eff} is the density of the pure compounds, C the Cunningham correction factor, χ the dynamic shape factor and d_{me} the volume equivalent diameter. ρ_{eff} is the effective density defined as:

$$\rho_{eff} = \frac{m}{d_{me}^3}\cdot\frac{6}{\pi}$$

Thermal Management, Design, Performance and Verification (SINTEF)

Introduction

During the *SootSens II* project, a continuation on the thermal design first developed in the *SootSens I* project has been a focus area. The design was further developed and experiments for verification purpose was performed.

Since the soot sensor concept relies on enhanced deposition of particles on a cold surface by thermophoresis, the thermal design is a crucial component in the system. The performance in the low temperature range ($T_{exhaust}$ < 100°C) of the thermal design has been a primary focus, since the proposed design is generically limited by the available temperature gradient between the ambient and the exhaust. At low temperatures the dew point of water limits the minimum sensor surface temperature. These two properties call for an efficient thermal design in the low temperature operation range.

The thermal design concept was patented by Sinvent AS (SINTEF) in 2009, patent application No. 2009 2713. In 2010 Sinvent has decided to secure further international patents rights (PCT).

The results were presented at the IEEE Sensors 2010 conference in November 2010. The paper may be found in the conference proceedings available at the IEEE Xplore website. The results also got attention in the December issue of the Norwegian magazine GEMINI.

Sensor design

This section describes how the thermal design works with basic principles. The thermal management system consisted mainly of a 140mm long heat shield made of copper. Its wall thickness was 2mm and its outer diameter was 12mm. The sensor substrate sticks through the heat shield protruding 5mm into the exhaust flow exposing the sensor surface. The back side of the protruding part is encapsulated with a copper cap to improve the local thermal performance at the region close to the sensor. The cap was welded to the heat shield top surface. The heat shield was thermally insulated from the exhaust pipe walls by a 10mm thick aluminum oxide ceramic paper. Illustrations of the setup are shown in Figure 14 and 15. The figures also show the different heat paths in the system.

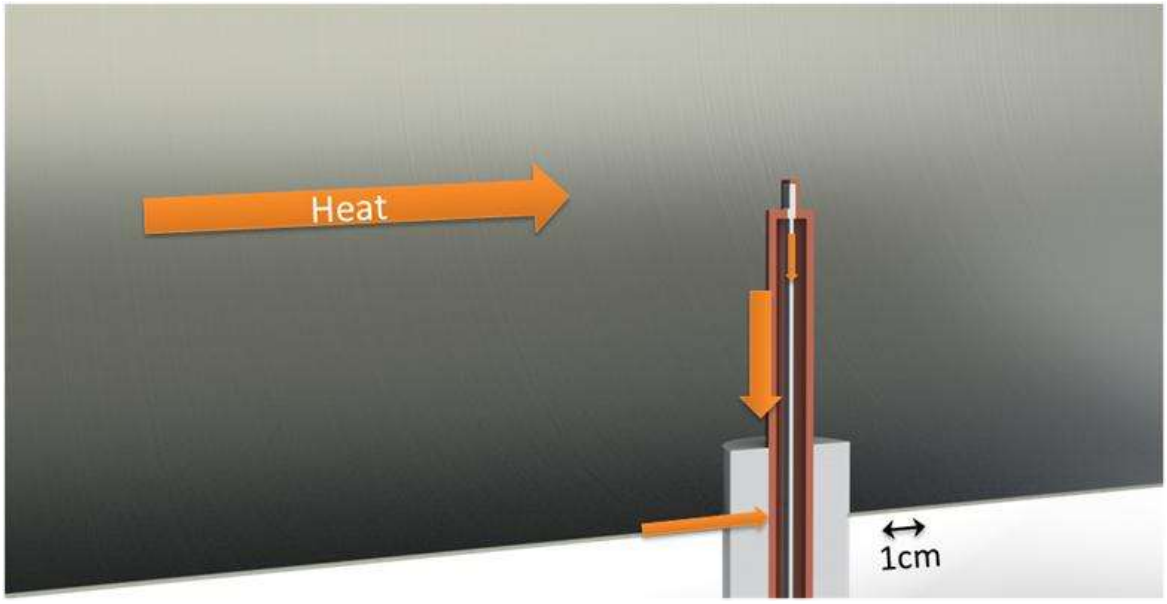

Figure 14. Device design. Exhaust flow is from left to right. Orange arrows illustrate the different heat paths in the system.

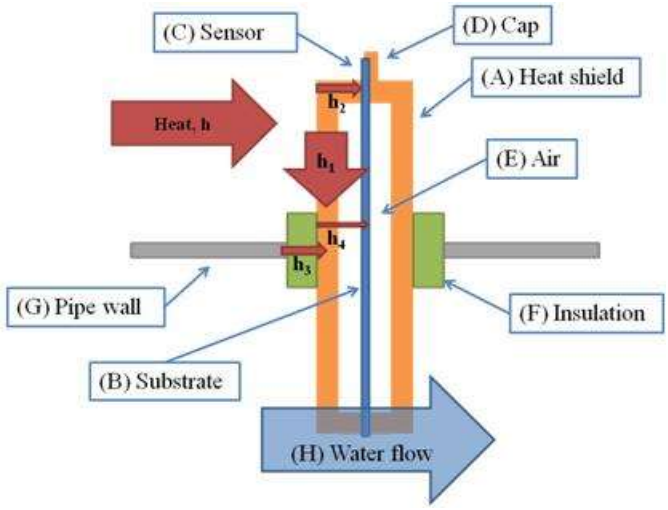

Figure 15. Concept drawing of the device design for the experimental setup.

The design works by shielding unnecessary large surfaces of the sensor substrate from direct exposure to the hot exhaust. The heat shield also provides the heat with a heat path of low thermal resistance. Heat entering the system mainly flows through heat paths with low thermal resistance; hence, by providing a path with very low thermal resistance, i.e. through the heat shield, compared to the heat path through the sensor substrate, the majority of heat will never reach the substrate. This enables compact and low cost cooling systems, e.g. ambient air cooling by forced convection, at the exterior region of the device. It also improves the acceptable ambient temperatures for a reliable operation, i.e. higher ambient temperatures are possible.

Simulations

The FEA was performed with COMSOL Multiphysics 4.0 utilizing the optional 'heat transfer' module package. FEA was used during the complete design process.

Physical conditions The flow characteristics were modeled with compressible flow with the k−ε turbulence model. To reduce model size, symmetry was used. The pipe wall was excluded from the model to further reduce model size, since it is not significant for the results for this type of system, as showed in the *SootSens I* project. All models were modeled as quasi−stationary systems.

Materials The material properties used for the finite element models (FEM) are presented **Table** . Properties of air from COMSOL material library was used to model the exhaust and the air inside the thermos.

Table 2. Material properties for finite element models.

Part	Density ρ [kg/m3]	Thermal Conductivity k [W/(mK)]	Heat capacity Cp [J/(kgK)]	Ratio of specific heat γ	Dynamic viscosity μ [Pa*s]	Surface emissivity ε
Adhesive	2650	0.72	1000	-	-	-
Substrate	3750	20[a]	900	-	-	0.05/0.95
Heat shield	8960	401	384	-	-	0.5[a]
Insulation	192.1	0.06[a]	1046.7	-	-	-
Exhaust/Air	1.2[a]	0.03[a]	1020[a]	1.4	1.8−5[a]	-

[a]Characteristic value for nonconstant material properties that depend on T, P or both.

Finite element model sensitivity The model sensitivity to mesh and material parameters was checked for all models. Quadratic tetrahedral elements were used. A typical mesh is shown in Figure .

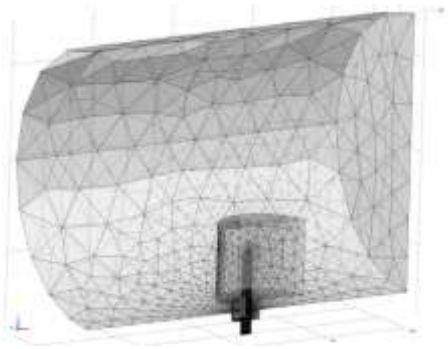

Figure 16. Typical mesh used for the FEA.

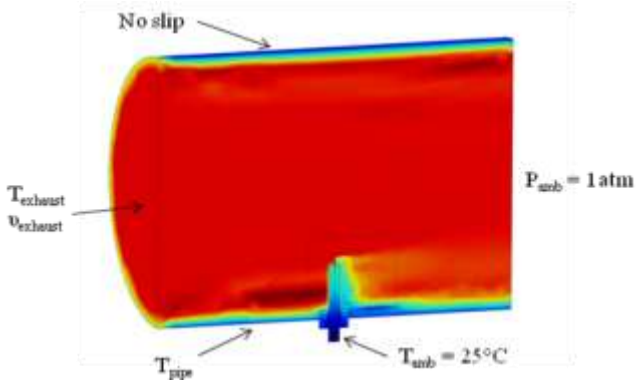

Figure 17. Typical BC used for the FEA.

Boundary conditions Typical boundary conditions (BC) used for the FEA are presented in 17. The pipe wall temperature was estimated to be between 20°C and 160°C during operation. The pipe and exhaust temperature combinations used is shown in **Table** . The exhaust speeds were modeled from 0.01m/s up to 10m/s to investigate the forced convection properties of the system. One model was checked for presence of natural convection inside the thermos. Remaining models were modeled without the fluidic properties of air inside the thermos, i.e. without convection. Two models were modeled with radiation between heat shield and sensor substrate. The emissivity of the substrate were set to ε=0.95 and ε=0.05, representing a surface with either high or low absorption of thermal radiation.

Table 3. Combinations of boundary conditions for exhaust and pipe temperatures.

Location	**Temperature [°C]**							
Exhaust	50	75	90	100	150	200	300	400
Pipe	20	30	36	40	60	80	120	160

Experiments

For the experiments, SINTEF constructed a flow loop that was able to produce turbulent wind speeds up to 10m/s and gas temperatures extending from room temperature up to 300°C. The flow loop had a 300mm inner diameter. The sensor device was placed into an adapter with a temperature controlled water flow. The water flow was used to control the external temperature keeping the temperature as similar as possible to the simulation setup. It also mimics an external forced convection cooling intended for a real diesel exhaust system. A picture of the tested sample is shown in Fig. 18.

Figure 18. Soot sensor set up for testing of thermal management design

Sensor Packaging (Mandalon Technologies AB)

The intention from the beginning was to make a general sensor rod in order to be able to adjust the components afterwards. This led to a complex structure with some drawbacks. As described in previous chapter we implemented backside heaters, around-sensor heater and several wire bondable connection points. This complexity led to narrow conductors and thus too high resistivity. For the first batch this has been taken care of through bypass wiring in order to reach low enough resistivity for the measurements. From a packaging point of view this path is working but unreliable and also time consuming.

The experiences from batch 1 have led to the design of batch 2 which has focused on basic function of the sensor, rear side heater and temperature measurement points.

All packaging considerations have to deal with the elevated temperature in exhaust pipes and to obtain the desired temperature gradients. Most of the electrical connections has been made with gap welding and, when applicable, normal soldering on colder areas. All attachments have been made with ***Resbond 907 GF***, a glass fibre reinforced putty designed for exhaust systems. However, due to the small system dimensions there is room for improvement as the fibres becomes comparatively large. All internal connections are secured with Resbond.

For the first measurements the sensor rod was mounted bare as in Fig. 19.

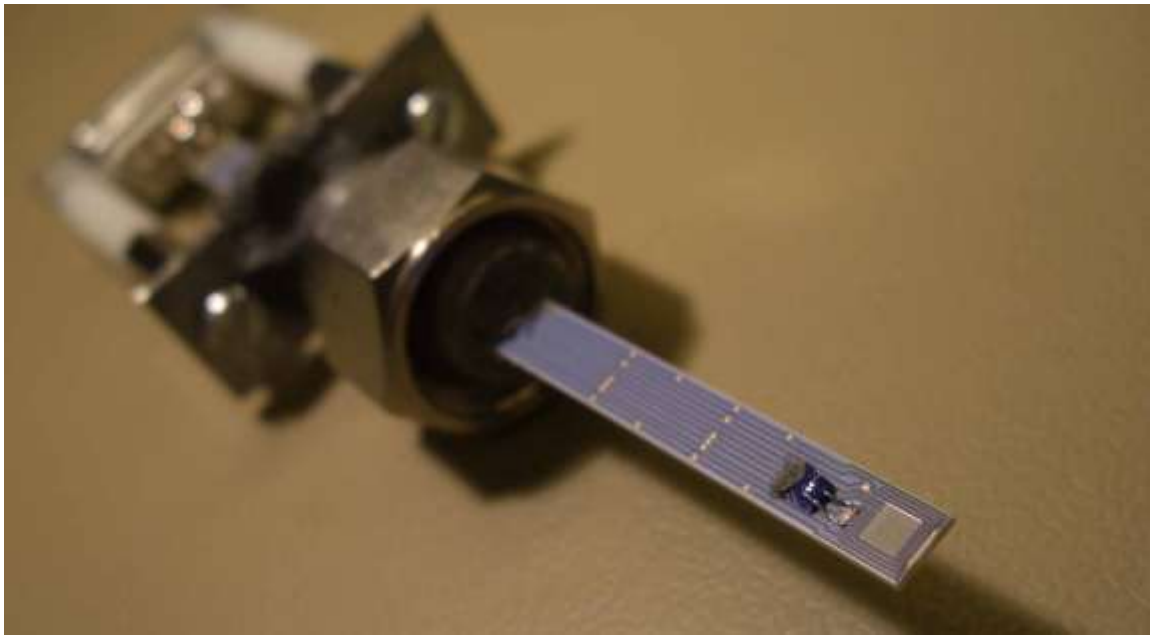

Figure 19. Bare sensor rod with Pt-100 attached

The later design for the whole component is made in accordance with the thermal simulations as a “thermos”. The thermos is built with 10 mm diameter stainless tubes of varying lengths, the sensor rod centered in the tube and fitted with the ceramic putty. The bypass approach lets us also apply temperature sensors, Pt-100’s, along the rod, inside the tube. We have also tested an active cooling of the sensor tip. This is performed with an applied air flow beneath the sensor tip, see Fig. 20.

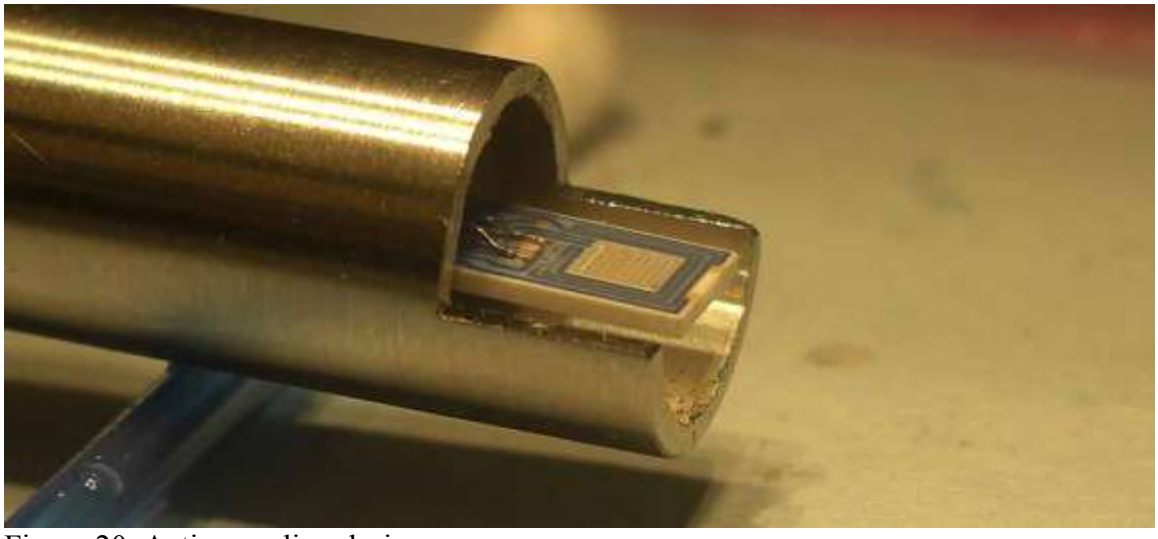

Figure 20. Active cooling design

In order to regenerate the sensor we need to heat the tip. This is made with a Heraeus heater mounted on the back of the sensor tip. At the back end all electrical connections are made thru a D-sub connector.

Figure 21. Test of heated tip of sensor rod

Fig. 22. Electrical connections

Sensor Electronics (SINTEF, LiU)

SINTEF have tested the electronics required to control the sensor in a cyclic operation between soot capturing and regeneration. An off-the-shelf integrated circuit specified for automotive applications has been identified as a key component for this purpose. An electronic test board based on this component has been developed. The cyclic mode is shown schematically in the graph below. The x-axis show the resistance of the SootSens sensor and the y-axis show the voltage signal read by this integrated circuit.

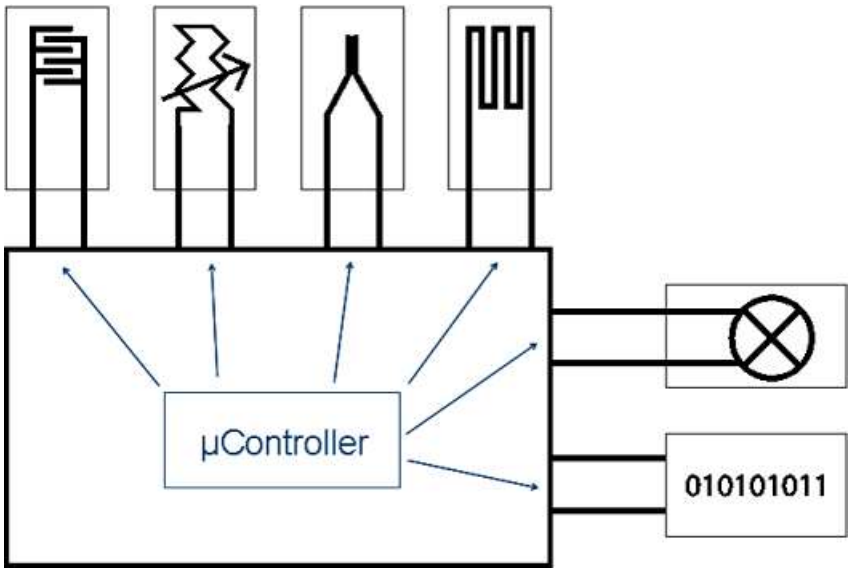

Fig. 23. Schematic picture of the electronics for the soot sensor system including soot sensor, Pt 100 temperature sensor, thermoelement, heater and microcontroller.

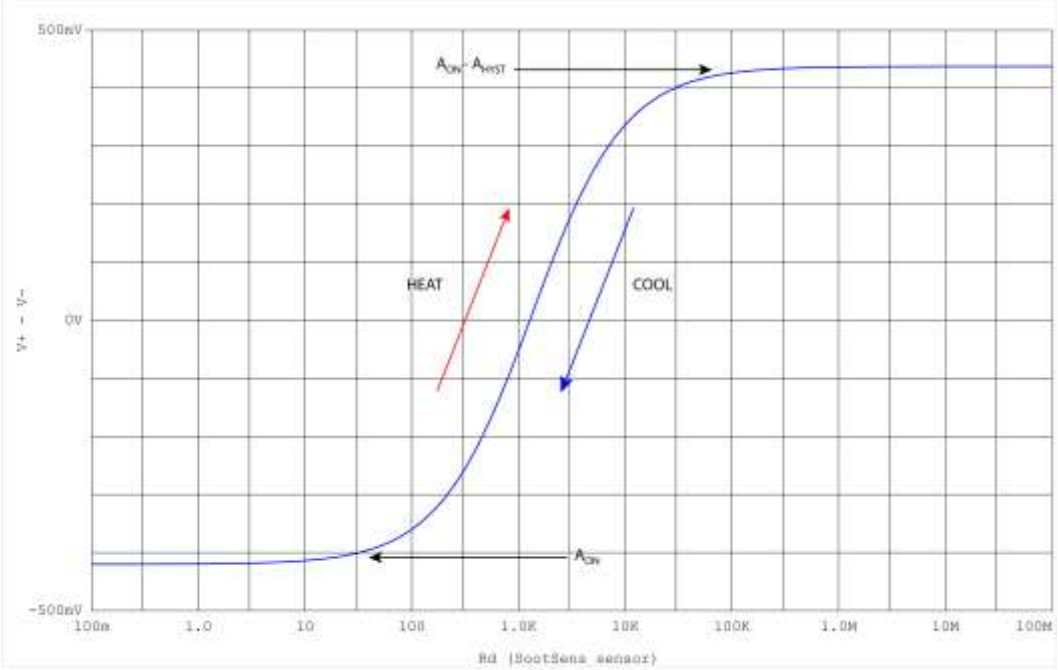

Figure 24. Voltage versus resistance of the soot sensor operated in a two temperature cyclic mode.

This first prototype is large and bulky and only suitable for proof-of concept measurements in the laboratory, see Fig. 24. The final electronics will of course be much smaller and integrated in the sensor system.

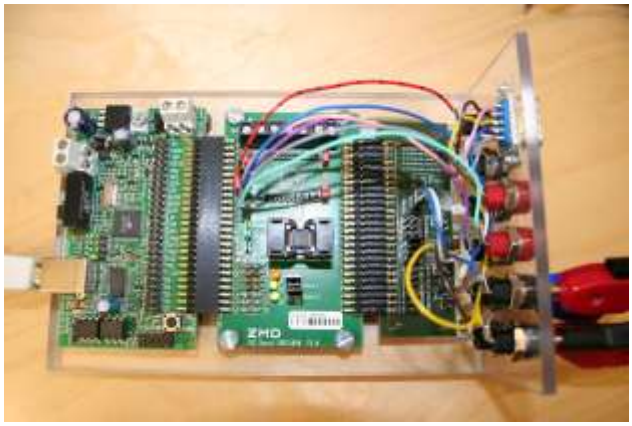

Figure 25. The electronics for cyclic temperature operation of the soot sensor

Some problems remain to be solved in order to use this standard equipment for the soot sensor in this project. SINTEF has had rather limited financial resources in the project and therefore has focused on the Thermal management simulation, which at this stage in the project was the most important. For the testing in diesel exhausts at VOLVO the necessary electronics was therefore developed at LiU.

Sensor Testing in the laboratory (LiU, ULUND)

Soot generation – stability and characterization

One of the aims of this investigation was to produce a set of soot particle size distributions and concentrations with high stability. Average particle size distributions used for the deposition experiments are shown in Fig. 25 a**.**

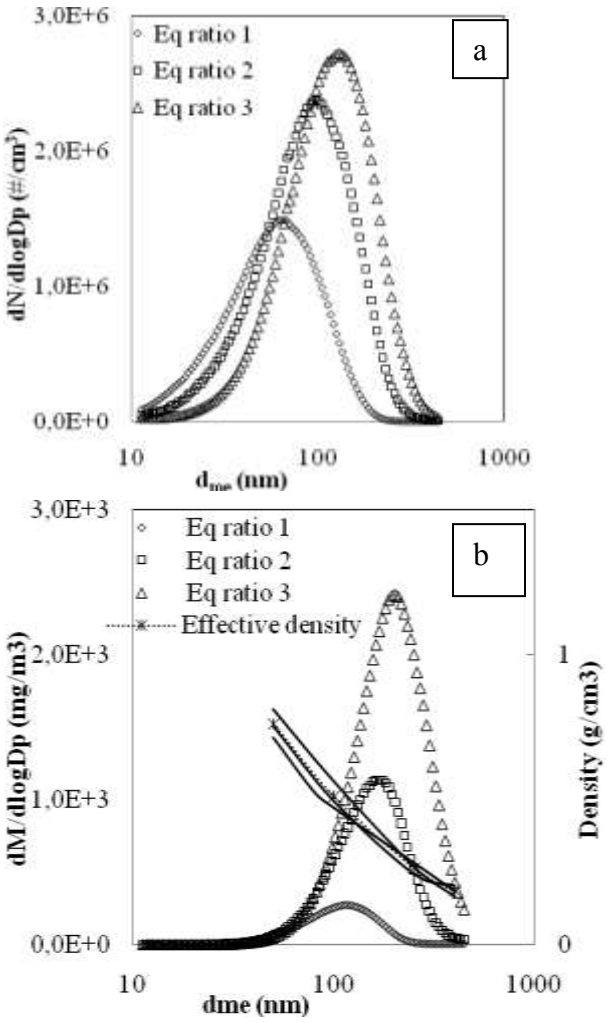

Figure 25: SMPS measurement of number and mass distributions

All distributions are unimodal, with slight deviations from lognormal distributions. The geometric mean diameters (GMDs) based on number concentration were 55, 85 and 110 nm and the geometrical standard deviations (GSDs) were 1.77, 1.80 and 1.81 respectively for the three cases. The smallest GMD (55 nm) is considered to be similar to a typical diesel soot size distribution.

The effective density of soot particle was also measured using the DMA-APM technique. The effective densities for a given size varied by less than 10% for the three different equivalence ratios. The effective density decreased with increasing particle size from ~0.8 g/cm3 for 50 nm particles down to below 0.2 g/cm3 for 400 nm particles. The results are presented in Fig. 25 b.

The first sensor testing by thermophoresis

A simple deposition cell where a thermal gradient was established between the sensor surface and the gas stream was constructed. Since thermophoretic deposition of the soot particles was favored by the contact of the gas flow with a cold surface, the diluted soot flow was heated to 240-270^{o}C before deposition by passing it through a steel coil heated by an electrical heater. The finger electrode sensor was heated by the gas stream and the temperature, as measured by the Pt 100 sensor, was in the range 105-125°C. These temperatures were sufficiently high to prevent water condensation at the dilution levels used. Soot layer morphology was investigated by SEM using a Leo 1550 VP emission field scanning electron microscope, see Fig. 26.

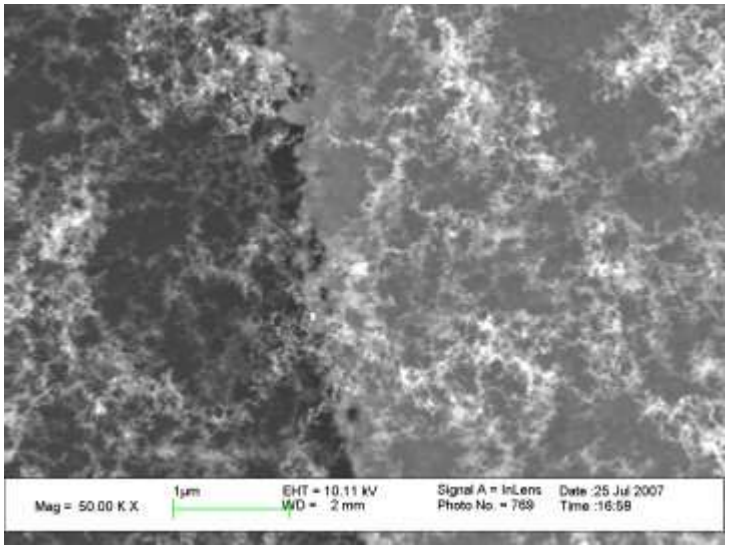

Figure 26. Typical SEM image of soot deposited onto SiO_2 (dark grey, to the left) and the gold electrode (grey, to the right)

For sensing purposes, the deposition of soot leads to formation of multiple disordered bridges between the metallic fingers creating a conductive layer as stipulated by the perculation theory. Since initial deposits are insulated from one another, a delay is expected before a resistance decrease is registered. The resistance measurements were performed using a multimeter device (TTI 1604) capable of measuring in the resistance range from1 kOhm to 20 MOhms. The time delay for the initial resistance decrease as well as the total resistance decrease was observed to be dependent on the distance between the metal finger electrodes as shown in Fig. 27.

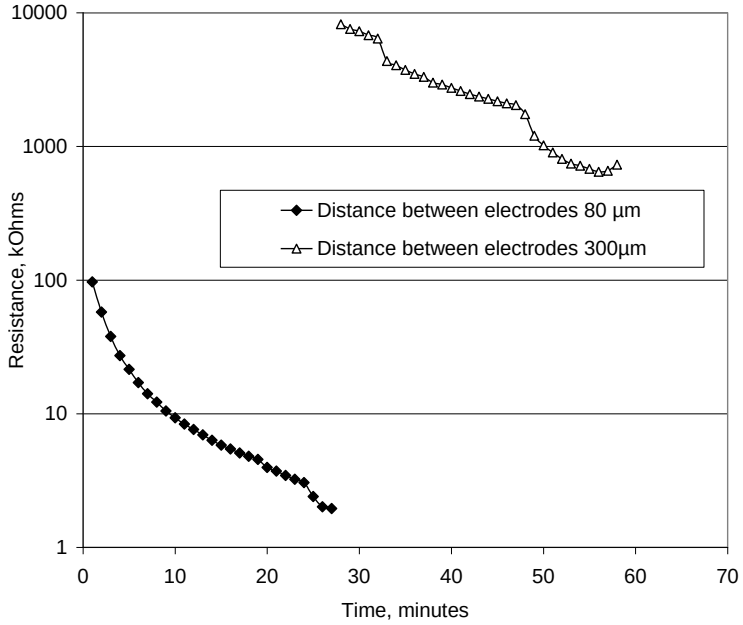

Figure 27. Resistance values evolution in time for different distances between electrodes - logarithmic scale (dilution ratio: 1/100; gas flow temperature: 240°C, sensor temperature: ~ 100 - 125°C)

Improved deposition by thermophoresis and resistivity measurements

As the soot particles, which contain conducting elemental carbon, deposit on the sensor surface they will start building a network of disordered bridges in the gaps between the metallic fingers until the first conductive layer is established. This process will take a certain time (referred to as on-set time) where no resistance decrease is recorded. There will also be a certain time before the resistivity decreases enough to fall into the measureable range of our measurement system.

Figure 28 shows the electrical resistance over time when depositing soot generated with equivalence ratio 1 (55 nm), 2 (85 nm) and 3 (110 nm) on fresh sensors continuously for 2h. Before the first conductive layer of soot was established on the substrate surface, the resistance values between the finger structures were out of the measurable range and set to the maximum measuring range in Fig. 28, 40 Mohms. The figure shows a significant difference in on-set time between the three different soot size distributions. The on-set times of 27.0, 7.0 and 1.6 minutes were observed when exposed to soot using three different cases of equivalence ratios 1, 2 and 3 (GMD = 55, 85 and 110 nm), respectively. After that time, the resistance started to decrease as indicated by the multimeter. Different exposed soot size distributions did not only show a difference in the on-set time but also in the resistance levels during later part of exposure time, which continued to slowly decrease. For equivalence ratios 2 and 3, the resistance profile seems to be similar, starting with a relatively fast decrease for the first 20 min and then beginning to almost level off, reaching a final resistance of 34 and 8 kOhm for set exposure time, respectively.

For the equivalence ratio 1 case, the resistance profile follows a smoother decline ending up at a considerably higher resistance of close to 1 Mohm.

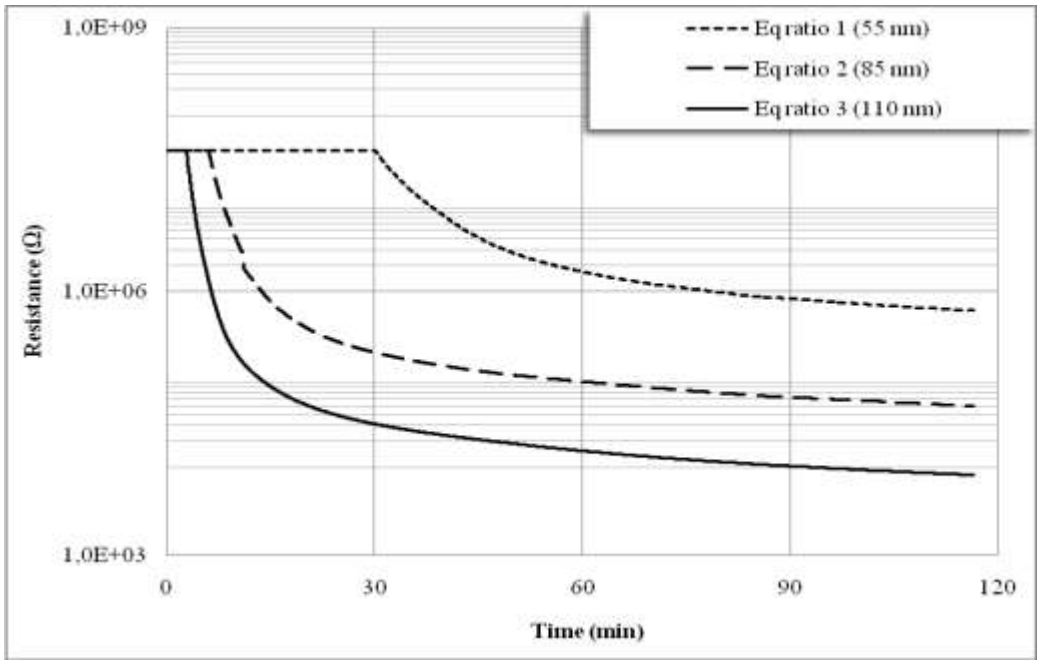

Figure 28: Examples of a single measurement showing the resistance change over time for fresh sensors exposed 2h to generated soot particle modes with GMDs of 55, 85 and 110 nm, respectively.

The difference in resistivity and on-set time can largely be explained by different mass exposures per minute for the three different cases. After normalization of the resistivity with cumulative mass-exposure, the three curves appeared more similar, see Fig. 29. Still, there was a difference in resistivity between the cases: The case with the largest agglomerate mobility size (110 nm) showed the fastest decrease in resistivity. There are several possible reasons for this: The particles in the size distribution with GMD = 55 nm are more compact as shown by the higher effective density compared to 85 nm and 110 nm. Depositing a larger number of more compact agglomerates, compared to fewer larger agglomerates with more open structures but with the same total deposited mass will require a longer on-set time as it will take longer to create an electrically conducting bridge between the electrodes. One can expect that the fractal-like conducting branches between two electrodes are being longer for the cases of larger agglomerates as an effect of the decreased effective density. However, it is interesting to note that the relative difference between the three cases increases with time.

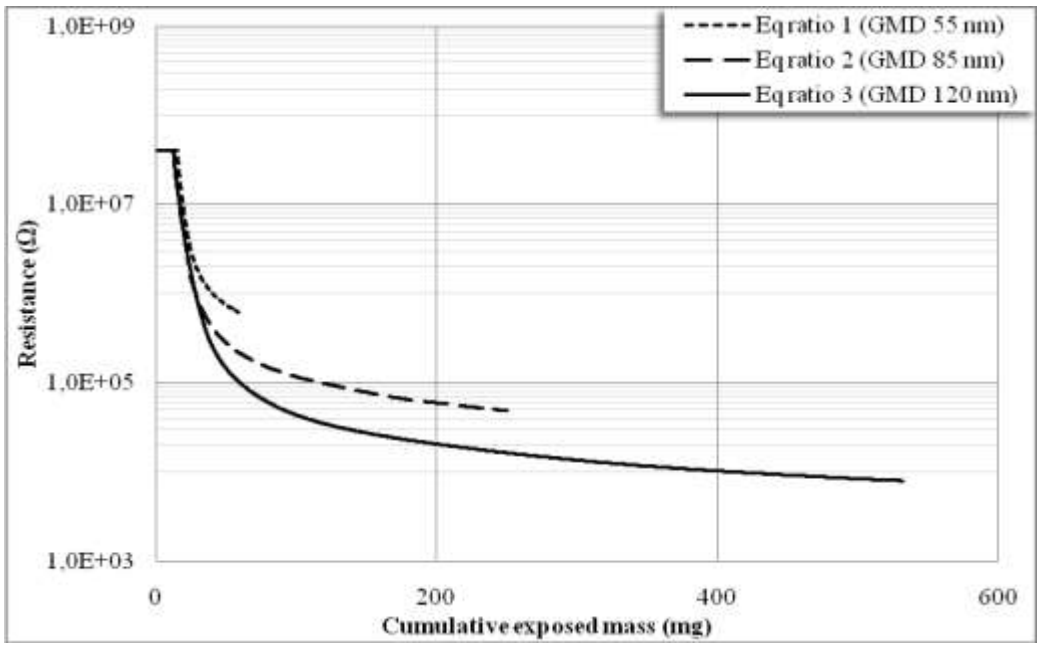

Figure 29: Experiments showing the cumulative mass of soot exposed and the resultant change in resistance for fresh sensors for 2h test by particles with GMDs of 55, 85 and 110 nm.

Sensor testing in diesel exhausts (LiU, VOLVO)

In gas streams having variable temperature the usual mode of operation for gas sensors requiring constant temperature is to establish a constant working temperature above the maximum in the ambient. This mode of operation is not available for operation of particle sensors because of the antithermophoretic effect which would prevent particles from reaching the sensor surface. For this reason we have adopted a passive cooling strategy for the sensor where heat dissipation from the interdigitated electrode sensing area was along the alumina substrate to outside the exhaust pipe. The physical set-up is illustrated in Fig. 29 and on the left-hand side of Fig. 30, where the tube insulating the sensor substrate is shown extending into the exhaust pipe with the sensing electrodes positioned in the center of the gas flow. A thermal situation is shown in the right-hand side of the figure where heat from the flowing exhaust gas is conducted from the sensing electrode area along the substrate to be dissipated both to the pipe wall and external environment. This heat dissipation maintained the sensing electrode area at a lower temperature than the ambient exhaust gas environment at all conditions. Simulations indicated that for exhaust gas temperature of 300°C the sensing electrode area was maintained at about 175°C using the tube thermos design as the thermal management solution.

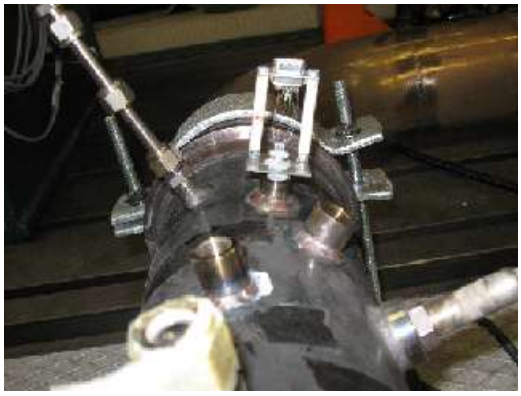

Figure 29. Outside view of the exhaust system with the SootSens sensor and other prototypes for testing at VOLVO.

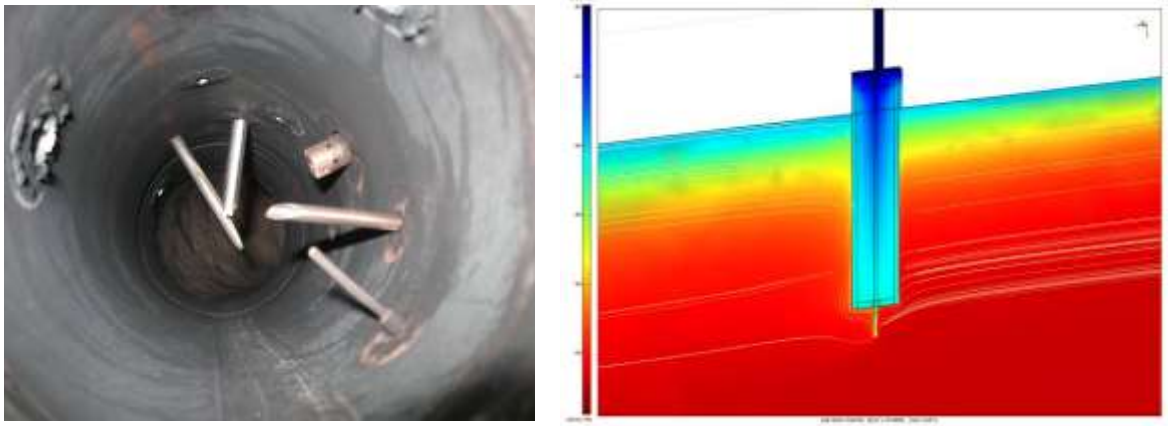

Figure 30: Inside view of sensors positioned in exhaust pipe (left) and simulation of temperature gradient of the SootSens sensor with thermos packaging (right).

The sensor housing was designed to insulate the substrate from the exhaust gas stream in order to enhance heat dissipation along the substrate. An example of the cooling achieved at actual exhaust conditions is shown in Fig. 31. Temperature sensors were positioned on the sensor rod close to the active finger electrode area and in the middle of the thermos tube for comparison. Increasing the speed and load on the motor caused the exhaust gas temperature to increase. The temperature difference between the exhaust gas and the electrode sensing area increased with increasing exhaust temperature reaching a maximum of about 150°C when the exhaust was about 470°C. The temperature of the sensing electrodes at exhaust gas temperature 300°C was about 230°C which is considerably higher than the 175°C calculated in the simulation. The two key parameters in the simulation, exhaust gas flow and pipe wall temperature, are difficult to control experimentally which was the probable cause of the discrepancy.

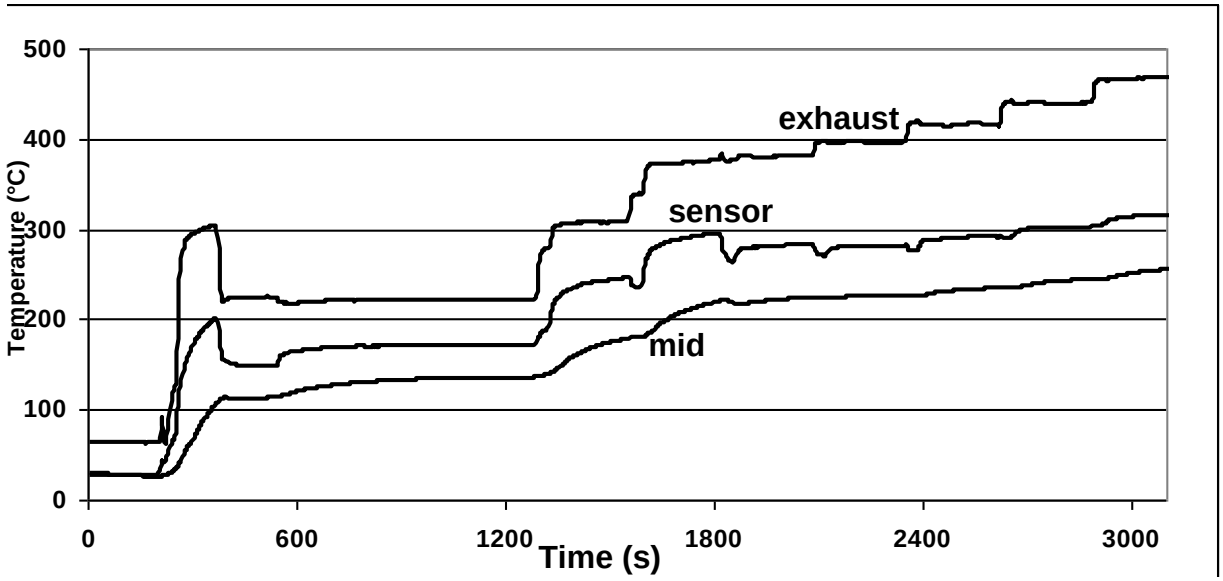

Figure 31. Exhaust gas, sensor and midtube temperatures during increasing speed and load on a marine motor.

Since the sensing mechanism is based on filling the empty space between the fingers of the interdigitated electrodes with a conducting network of soot there was an incubation time involved in the sensor response before a resistance decrease was observed. This has been called percolation time [27] with reference to the well-known effective medium theory of how conducting particles in an insulating matrix control overall electrical conductivity. This percolation time has been shown to be reproducible at constant exhaust gas temperature and soot concentration during several sensor regeneration cycles and thus could be used as a parameter to monitor soot in exhaust gas.

Experiments were done to determine if the rates of resistance decrease which follow soot accumulation on the sensor after the percolation threshold was reached correlated with soot concentration in the exhaust gas. A constant exhaust gas temperature of 200°C was established by setting the speed and load on an automobile motor at 1700 rpm and 40 newtonmeters. Passive cooling of the sensing electrode area established the sensor temperature at about 40°C lower than the exhaust gas at these conditions. The collection/burn-off cycle when the soot concentration was 4 mg/m^3 is shown on the left-hand side of Fig. 32. A resistance decrease from 101 to about 20 MΩ after the percolation threshold was reached was followed by a burn-off period which restored the sensor resistance to the101 MΩ level. Measurement/burn off cycles were repeated five times at this concentration and the curves are shown in the right-hand of Fig. 32. The procedure was repeated for two additional soot concentrations, 7 and 10 mg/m^3, obtained by increasing the air intake to the motor. The average curves from these measurements are shown in the left-hand side of Fig. 33. There was an inverse relationship between soot concentration and the time required to reach 20 MΩ resistance.

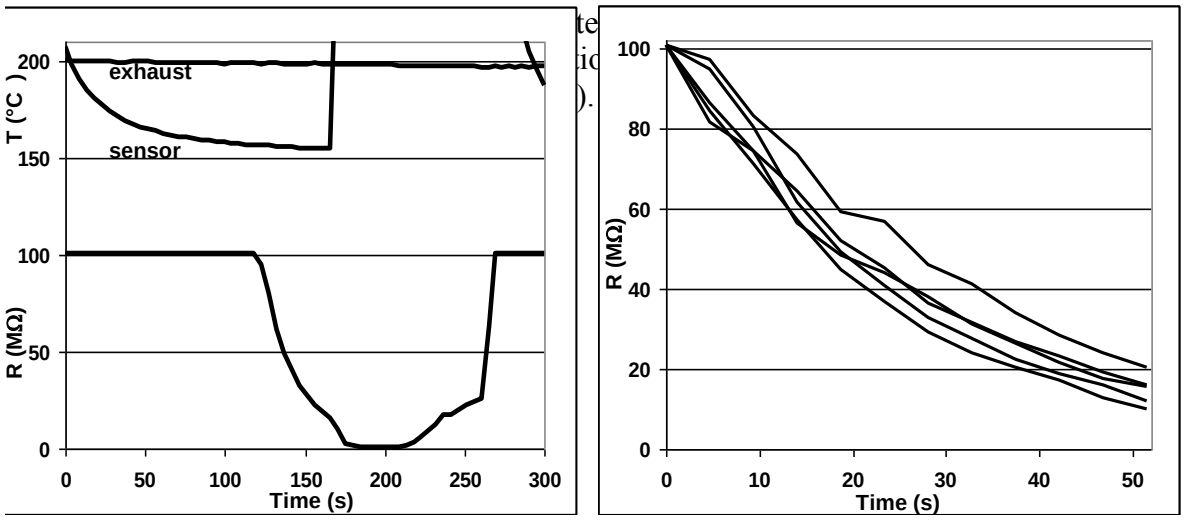

Figure 32. Exhaust gas temperature, sensor temperature and resistance during a collection/burn-off cycle for soot concentration 4 mg/m3 (left) and five resistance decrease curves at the same condition (right). Sensor temperature was increased to 600°C at 170 s.

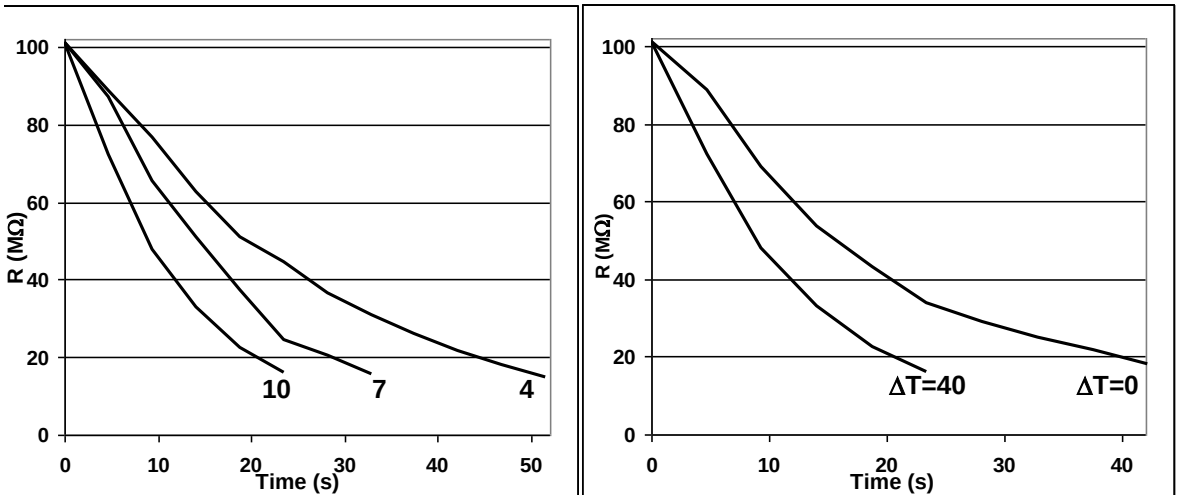

Figure 33: Averages of 5 resistance decrease curves for 4, 7 and 10 mg/m3 soot concentrations (exhaust temperature 200°C, sensor temperature 160°C) (left) and resistance decrease curves for soot concentration 10 mg/m^3 with the same 40°C temperature difference between exhaust gas and sensor and with no temperature difference (right).

The time to reach the measureable resistance change has been proposed as an additional parameter related to the gas phase soot concentration. For the concentrations 4, 7 and 10 mg/m^3, the average percolation times from when the sensor temperature went below 200°C until the resistance decreased below 101 MΩ were 108, 104 and 97 s, respectively. There was thus some correlation between percolation times and soot concentrations. However, the experimental conditions were not ideal for determining the percolation time. In order to maintain constant exhaust gas temperature, it was necessary to vary the air

intake to the motor to obtain different soot concentrations. It required about 30% more air to decrease the soot concentration from 10 to 4 mg/m^3 and this resulted in different passive cooling rates for the sensor. Since the central theme of this report is how the temperature difference between sensor and exhaust gas affect soot accumulation, there was thus some uncertainty in the percolation times based on the variations in cooling rates from 200 to 160°C.

The effect of the temperature difference was investigated by warming the sensor at 200°C during soot collection and the result for the 10 mg/m^3 soot concentration is also shown in Fig. 33. A 20 s faster decrease to 20 MΩ was observed for soot collection with a temperature difference between the exhaust gas and sensor of 40°C. The average percolation time for the sensor cooled to 160°C was 108 s as compared to 152 s when the sensor was warmed to the exhaust gas temperature. Passive cooling of the sensing electrode area thus decreased the percolation time and increased the rate of resistance change. Since electrical conductivity is a thermally activated process, it was the faster soot collection rate at the lower temperature which caused the faster responses. This may have been from an increased contribution of thermophoretic soot deposition in the deposition process.

The curves for the three soot concentrations shown in Figs. 32 and 33 represent the resistance changes upon soot collection on the sensor for the specific steady state conditions of exhaust gas temperature 200°C. This sort of condition could be achieved during highway driving at constant speed. But most vehicle use involves frequent accelerating and braking which results in constantly varying temperatures in the exhaust gas. For this reason vehicle parameters such as fuel consumption and emission certification are obtained by running engines at specified load patterns and duty cycles. These driving cycles vary in different global regions. One such cycle is the World Harmonized Transient Cycle which has been created to cover typical driving conditions for heavy duty vehicles in the EU, USA, Japan and Australia. The test takes 30 min and includes several motoring segments to simulate both city and highway driving conditions. The hot start version of the test was chosen to test the sensor's ability to detect a crack in a particulate filter which was simulated by drilling a hole in the center of a recently regenerated filter.

Fig. 34 shows results for sensor response and regeneration during six consecutive transient cycles. Each cycle was started when the exhaust gas temperature reached 200°C as a result of applying a speed and load to the engine. At the conclusion of each cycle the engine was idled until the temperature in the exhaust gas decreased to <100°C. Sensor performance indicated a percolation time followed by resistance decrease to <1 MΩ. Regeneration of the sensor was started at the finish of each cycle by raising the temperature to 600°C and finished by turning off the heater when resistance had returned to 1 GΩ.

Average total soot passing through the filter during each cycle was 1370 mg (40 mg/kWh based on engine effect). Average percolation time for five of the cycles was 18 min. Cycle 4 had a much shorter percolation time of 7 min. This could have been caused by

macroscopic soot covering the sensing electrodes. Soot tends to accumulate at cracks in the filter and such accumulations can dislodge and pass through the exhaust pipe. It is also possible that the regeneration of the sensor surface was incomplete before the start of cycle 4. The jagged resistance curve prior to reaching 1 GW for regeneration 3 may indicate that the heater was turned off before all soot had been removed which resulted in the final resistance increase being caused by the decreasing temperature. Soot remaining on the sensing electrode area prior to the start of cycle 4 would have decreased the percolation time necessary to start the following resistance decrease.

Speed and load on the motor during the cycle was greatest during the final 10 min segment representing constant speed highway driving. The temperature difference between the sensing electrode area and exhaust gas was maximum during that segment but soot accumulation toward the percolation threshold also occurred during the lower temperature variable speed segment.

Fig. 33 indicates one possible application for resistance type soot sensors, detection of malfunction of the particulate filter as evidenced by an increase of soot downstream from the filter. Since this type of application doesn't require that the sensor follow the real-time fluctuations of soot concentration in the exhaust gas, only indicate when it is raised over a period of time or driven distance, it is well suited to the cyclic mode of sensor operation. Compare the proposed California Code of Regulations Title 13, Section 1971.1.e.8 requirement for OBD of the particulate filter after 2013 where all types of deterioration or failures must be detected before tailpipe emissions exceed 0.03 g/BHP-hr=0.04g/kWh (BHP=brake horse power, engine horse power without loss caused by auxiliary components). The average soot concentration/kWh based on the engine effect during the cycles was thus at the level which should be detected for OBD of the particulate filter function. The OBD detection limit may in the future be expressed in terms of driven distance. In practical terms the method of filter malfunction detection by resistance sensors may be accomplished by monitoring the sensor regeneration frequency. A resistance sensor positioned downstream of a properly operating filter would normally require infrequent regeneration. Any significant increase in the frequency of sensor regeneration would thus be an indication of possible filter malfunction.

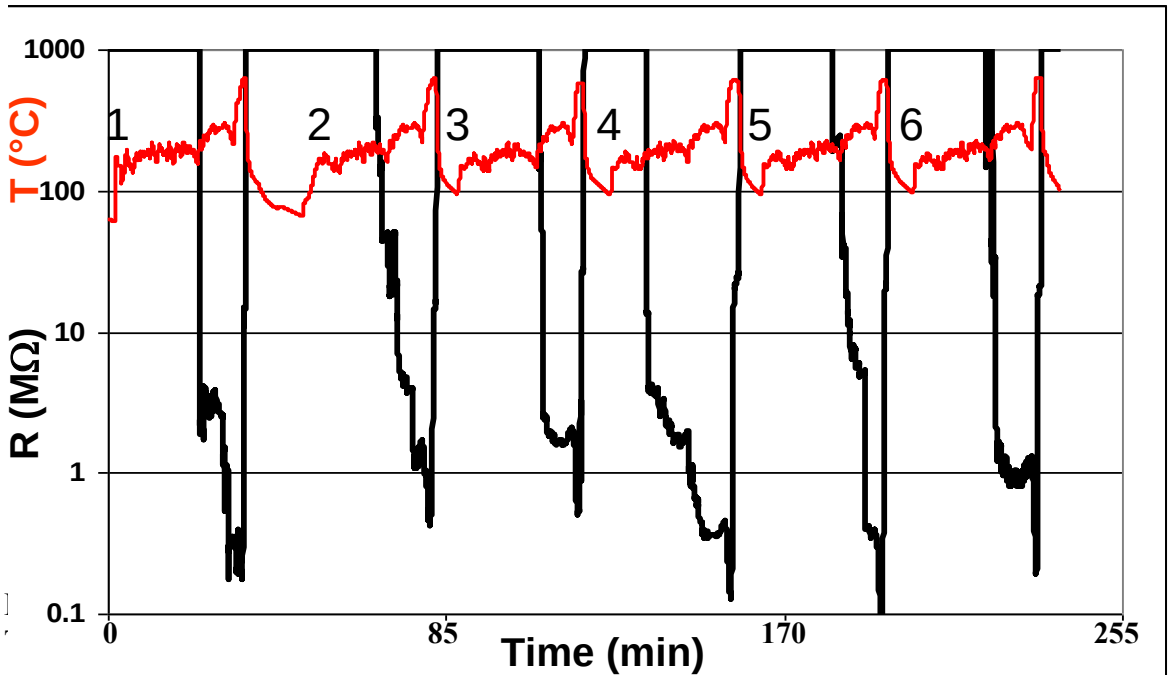

Figure 34: Sensor temperature (red) and sensor resistance (black) during six World Harmonized Transient Cycles. Each cycle was started when the exhaust temperature reached 200°C. The sensor temperature was increased to 600°C to burn off soot and the motor was idled after each cycle.

Conclusions

- We have qualitatively showed that thermophoresis is a viable sensor technology for soot detection with high sensitivity.
- A thermos concept for efficient cooling of the sensor surface has been demonstrated
- Transistor devices are interesting for soot detection
- Soot can be produced by aerosol technology for testing of sensors in the laboratory and calibration of soot sensors

Future

Further development of the soot sensors

A soot sensor project also proceeds within the VINN Excellence centre FunMat. Testing of transistor devices as well as further proof of concept regarding the influence of cooling of the sensor surface will continue within FunMat together with further testing of sensing layers for improved soot detection. The development in the FunMat centre regards advanced materials for the metal contacts of the soot sensor. Contacts are required, which are long term stable during cycling of the operation temperature between about 50 - 150°C below the diesel exhaust temperature and a regeneration temperature of about

600°C. The MAX materials are identified as especially interesting for the development of these contacts.

Development of nanoparticle sensors

The coordinator, Lloyd Spetz, started from January 1, 2011 a half time position at Oulu University in Finland as FiDiPro, Finnish Distinguished Professor. The project of this position relates to development of a portable detector in order to detect nanoparticles according to size, shape, concentration and content, since all these parameters have shown to influence their adverse health effect. The FiDiPro position and its project originates from contacts within the ERA NET projects SootSens I and II and the achieved results. This will be a much larger project, which will require extensive development of the technology. However, the new project will greatly benefit from the results and methodology built up in the soot sensor project.

Publications

Journal papers

Doina Lutic, JoakimPagels, Robert Bjorklund, Peter Josza, Jacobus H. Visser, AnnW. Grant, Mats L. Johansson, Jaska Paaso, Per-Erik Fagerman, Mehri Sanati, Anita Lloyd Spetz, Detection of Soot Using a Resistivity Sensor Device Employing Thermophoretic Particle Deposition, Journal of Sensors 2010, Article ID 421072, doi:10.1155/2010/421072.

A. Malik, H. Abdulhamid, J. Pagels, J. Rissler, M. Lindskog, R. Bjorklund, P. Josza, J. Visser, A. Spetz, and M. Sanati, Generation of diesel like soot particles and thermophoretic deposition on resistivity soot sensor, Aerosol Science and Technology, 45:1–11, 2011

H. Bladh, J. Johnsson, J. Rissler, H. Abdulhamid, N.-E. Olofsson, M. Sanati, J. Pagels, P.-E. Bengtsson, Influence of soot particle aggregation on time-resolved laser-induced incandescence signals; Applied Physics B: Lasers and Optics, Volume 102 / 2011, pages not yet identified

Conference contributions

Doina Lutic, Eveline Popovici, Elena Seftel, Anita Lloyd-Spetz, Application of Some Micro- and Mesoporous Materials in Gas and Particle Sensing, First International Conference on Multifunctional, Hybrid and Nanomaterials, Tours, France**,** Abstract no. HYBR 1148, March 2009.

H. Abdulhamid, A. Malik, J. Pagels, Robert Bjorklund, Peter Josza, Jacobus H. Visser, Anita Lloyd Spetz, and M. Sanati, A Reliable Method for Generation of Size Selected

Soot using Aerosol Technology and Detection by Sensor Device, European Aerosol Conference 2009, Karlsruhe, Abstract T083A17.

D. Lutic, E. M. Seftel, E. Popovici, R. Bjorklund, M. Andersson, A. Lloyd-Spetz, Synthesis and characterization of catalytic siliceous materials with ordered structure for chemical sensors, European Conference on Applications of Surface and Interface Analysis (ECASIA 09), Antalya, Turkey, 2009, Abstract OXD-P-21 (819)+Tu-PA-194.

Andreas Larsson, Frøydis Oldervoll, Thermal modeling of a thick film based soot sensor for automotive applications, Proc. IMAPS Nordic 2009, Tønsberg, Norway, September 14, 2009.

Doina Lutic, Elena-Mihaela Seftel, Eveline Popovici, Robert Bjorklund, Mike Andersson, Hussam Abdelhamid, Mehri Sanati and Anita Lloyd Spetz, Synthesis of Catalytic Materials with Ordered Structure for Chemical Sensors, EuropaCatIX, Salamanca, Spain, September 2009, Abstract 1287.

R. Bjorklund, A. Grant, P. Jozsa, M. Johansson, P.E. Fägerman, J. Paaso, M. Andersson, L. Hammarlund, A. Larsson, E. Popovici, D. Lutic, J. Pagels, M. Sanati, A. Lloyd Spetz, Resistance sensor employing thermophoresis for soot in diesel exhaust, Proc. IEEE Sensors 2009, Christchurch, New Zealand, Oct 26-28, 2009 (poster).

R. Bjorklund, M.L. Johansson, A. Grant, P. Jozsa, P.E Fägerman, J. Paaso, A. Larsson, D. Lutic, A. Lloyd Spetz, Resistance sensor based on thermophoresis for soot in diesel exhaust, Proc. MRS Spring meeting, San Fransisco, USA, April 2010 (oral).

A. Malik, M. Lindskog, J. Rissler, J. Pagels, P. Nilsson, M. Bohgard, M. Sanati, Development of a High Temperature Aerosol Particle Sampling Probe for Field Measurements in Thermochemical Conversion of Biomass, in Proceeding of International Aerosol Conference 2010, Helsinki, Finland, 29 July -3 August. 2010; (No. 95)

R. Bjorklund, A. Grant, P. Jozsa, M. Johansson, P.E. Fägerman, J. Paaso, M. Andersson, L. Hammarlund, A. Larsson, E. Popovici, D. Lutic, J. Pagels, M. Sanati, A. Lloyd Spetz, Soot sensor based on thermophoresis for high sensitive soot detection in diesel exhausts, Proc. IMCS13, Perth, Australien 12-14 July, p. 250, 2010. **Invited talk**

Doina Lutic, Maria Ignat, Gina-Dumitrita Mihai, Elena-Mihaela Seftel, Eveline Popovici, Robert Bjorklund and Anita Lloyd Spetz, Pt-doped Mesoporous Semiconductive Oxides for Gas Sensing, Best Poster Award at the 1st International Workshop of the European Nanoporous Materials Institute of Excellence (ENMIX), entitled "Nanostructured Materials for Sorption, Separation and Catalysis"Antwerpen, Belgium, October 2010 (poster).

Doina Lutic, "Some Applications of Porous Materials in Gas and Particle Sensing", National Conference with International Participation: Nanostructured Multifunctional Materials, Iaşi, Romania, November 3-4th, 2010 (oral).

A. Lloyd Spetz, R. Pearce, M. Andersson, R. Bjorklund, R. Yakimova, D. Lutic, Nanostructured & porous materials for FET sensors, Nanostructured multifunctional materials, National Conference with International Participation: Nanostructured Multifunctional Materials, NMM, Iaşi, Romania, November 3-4th, 2010, **Invited talk**

Patents

PCT/SE2008/050215 Method and arrangement for detecting particles, Doina Lutic, Anita Lloyd Spetz, Mehri Sanati, Jaco Visser, Peter Jozsa, patent filed by Volvo CC (2008)

20092713/2009.07.20, Lokal termisk styring, SINTEF IKT, Andreas Larsson

References

1. D. W. DockeryDockery, Health effects of particulate air pollution. Annals of epidemiology 19:4 (2009) 257-263.
2. J. Hansen, L. Nazarenko, Soot climate forcing via snow and ice albedos. Proc. Nat. Acad. Sci. 101(2) (2004) 423-428.
3. D. S. Su, A. L. Serafino, J.-O. Müller, R. Jentoft, R. Schlögl, S, Fiorito, Environ. Sci. Technol**.** 42 (2008)1761.
4. A. Valavanidis, K. Fiotakis, T. Vlachogianni, Journal of Environmental Science and Health Part C, 26 (2008) 339.
5. S. Eidels-Dubovoi, Aerosol impacts on Visible Light Extinction in the Atmosphere of Mexico city. Sci. Tot Environm**.** 287, 3 (2002) 213-220.
6. T. C. Bond, R. W. Bergstrom, Light absorption by carbonaceous particles: an investigation review, Aerosol Sci. Technol. 40, 1 (2006) 27-679.
7. D. Jacob, Introduction to atmospheric chemistry, Princeton University Press, Princeton (1999). V. Ramanathan, G. Carmichael, Global and regional climate changes due to black carbon, Nature Geoscience 1 (2008) 221-227.
8. H. Burtscher, J. Aerosol Sci. 36 (2005) 896.
9. H. Patashnick, G. Rupprecht, US Pat 5279970, (1994).
10. H. Patashnick, G. Rupprecht, US Pat 5196170, (1993).
11. H. Schittenhelm, WO 2005/024400A1, (2004).
12. K. Wienand, M.Murziol, T.Asmus, K.Ullrich, A.Ogrzewalla, D.Teusch, WO 2006/111386 A1, (2006).
13. R. Sabine, O. Thorsten, K. Bernhard, H. Schittenhelm, WO 2006/077197, 2006.
14. M. Fleischer, R. Pohle, K. Wiesner, and H. Meixner, "Soot Sensor for Exhaust Gases", Eurosensors XIX, Barcelona (2005).
15. G. Fischerauer, M. Förster, R. Moos, Sensing the soot load in automotive diesel particulate filters by microwave methods, Meas. Sci. Technol. 21 (2010) 035108 (6pp)
16. W. C. Hinds, "Aerosol Technology: Properties, Behavior and Measurement of Airborne Particles", 2nd ed.; John Wiley and Sons, New York (1999); pp 54, 173 and 216.

17. R. Lorenzo R. Kaegi, R. Gehrig, L. Scherrer, B. Grobety, H. Burtscher, Aerosol Sci. Tech., 41 (2007) 934**.**
18. A. Messerer, R. Niessner, U. Pöschl, Aerosol Sci. 34 (2003) 1009
19. Directive 2000/53/EC - the "ELV Directive" Directive which aims at making vehicle dismantling and recycling more environmentally friendly, sets clear quantified targets for reuse, recycling and recovery of vehicles and their components and pushes producers to manufacture new vehicles also with a view to their recyclability. http://ec.europa.eu/environment/waste/elv_index.htm; read March 29, 2011.
20. M. Andersson, L. Everbrand, A. Lloyd Spetz, T. Nyström, M. Nilsson, C. Gauffin, H. Svensson, A MISiCFET based gas sensor system for combustion control in small-scale wood fired boilers, Proc. IEEE Sensors, Atlanta, USA Oct 28-31, 2007, 962-965.
21. M. M. Maricq, Chemical characterization of particulate emissions from diesel engines: A review. Journal of Aerosol Science 38, 11 (2007) 1079-1118.
22. J. Schneider, N. Hock, S. Weimer, S. Borrmann, U. Kirchner, R. Vogt, V. Scheer, Nucleation Particles in Diesel Exhaust: Composition Inferred from In Situ Mass Spectrometric Analysis, Environmental Science and Technology 39 (2005) 6153-6161.
23. A. Messerer, R. Niessner, U. Poschl, Thermophoretic deposition of soot aerosol particles under experimental conditions relevant for modern diesel engine exhaust gas systems, Journal of Aerosol Science 34, 8 (2003) 1009-1021.
24. C. J. Tsai, H. C. Lu, Design and evaluation of a plate-to-plate thermophoretic precipitator, Aerosol Science and Technology 22:2 (1995) 172-180.
25. R. Munoz-Bueno, E. Hontanon, M. I. Rucandio, Deposition of fine aerosols in laminar tube flow at high temperature with large gas-to-wall temperature gradients, Journal of Aerosol Science 36 (2005) 495-520.
26. P. H. McMurry, X. Wang, K. Park, K. Ehara, The Relationship between mass and mobility for atmospheric particles: a new technique for measuring particle density, Aerosol Science and Technology 36 (2002) 227–238.
27. C. Hagen, S. Feistkorn, A. Wiegärtner, D. Heinrich, R. Brüggemann, R. Moos, Conductometric soot sensor for automotive exhausts: initial studies, Sensors 10 (2010) 1589-1598.

norden

Nordic Innovation Centre

Nordic Innovation Centre

Nordic Innovation Centre (NICe) is an institution under the Nordic Council of Ministers facilitating sustainable growth in the Nordic economies.

Our mission is to stimulate innovation, remove barriers and build relations through Nordic cooperation. We encourage innovation in all sectors, build transnational relationships, and contribute to a borderless Nordic business region.

We work with private and public stakeholders to create and coordinate initiatives which help Nordic businesses become more innovative and competitive.

Nordic Innovation Centre is located in Oslo, but has projects and partners in all the Nordic countries.

For more information: www.nordicinnovation.net

Nordic Innovation Centre
Stensberggata 25
NO-0170 Oslo
Norway

Phone: +47-47 61 44 00
Fax: +47-22 56 55 65

info@nordicinnovation.net
www.nordicinnovation.net